

Measuring and mapping the impact of buffer width on riparian microclimate temperatures.

Thomas Reidy

School of Natural Sciences

Faculty of Science and Engineering

Macquarie University

Submitted 21/05/2023.

A thesis submitted in partial fulfillment of the requirements for the degree of Master of Research

DECLARATION

I declare that this thesis, as a whole or in parts, has not been submitted for a higher degree to any other university or institution. To the best of my knowledge and belief, the thesis contains no material previously published or written by another person except where due reference is made in the thesis itself.

No ethics approval was required for this project.

Thomas James Reidy

19/05/2023

Acknowledgements

I am very grateful to my supervisor Professor Kirstie Fryirs, who's guidance has been tremendously helpful throughout this research project. I truly appreciated all her advice, patience, encouragement and friendly attitude during this project and my undergraduate studies. The same is extended to my co-supervisor Associate Professor Peter Davies who always offered insightful advice along with a great smile around the office. I would also like to thank Jocelyn Dela-Cruz who helped shape the early elements of this project as well as providing some very useful sources on our study area of South Creek on behalf of the NSW Department of Planning, Industry and Environment.

Thank you to the hardworking people who joined me in the field, Aaron Panozzo, Elahe Mirabi and Nick Goodwin, as well as the black snakes who proved to be less trouble than the overly friendly horses. I am also grateful to the Mamre Homestead and Twin Creeks Country Club groundskeepers, staff, and landowners for allowing us to access and work on their land, as well as being accommodating and friendly along the way.

I acknowledge the Dharug people as the traditional owners of the land and the Wianamatta on which this research was.

Finally thank you to my friends, family and colleagues who have consistently being friendly, welcoming, and helpful.

This research was supported by a NSW Department of Planning, Industry and Environment research grant and Macquarie University Higher Degree Research Funds. I am also grateful for the support of a Macquarie University Research Excellence Scholarship (MQRES).

Contents

1.	Introduction, literature review and thesis aims	2
1.1	Introduction.....	2
1.2	Environmental benefits of riparian zones in urban streams.....	4
1.3	River Thermodynamics	5
1.4	Riparian Microclimate.....	6
1.5	Remote sensing and modelling.....	8
1.6	Thesis Aims and Objectives	10
2	Regional Settings and methods	11
2.1	Regional Setting	11
2.2	Site characteristics	12
2.3	Methodology.....	15
2.3.1	Sensor Placement.....	15
2.3.2	Data processing.....	16
2.3.3	Geoprocessing.....	17
3	Results.....	20
3.1	Riparian Microclimate	20
3.1.1	Daily maximum and minimum air temperatures.....	20
3.1.2	Air temperature gradients	24
3.1.3	Common distance air temperatures	25
3.1.3	Diurnal air temperature variation.....	27
3.2	Water Temperatures.....	28
3.2.1	Daily maximum and minimum water temperatures	28
3.2.2	Diurnal water temperature variation	31
3.3	GIS	32
3.3.1	Riparian vegetation inventory	32

3.3.3	Riparian Cooling	35
4	Discussion.....	38
4.1	Riparian Microclimate	38
4.1.1	Bankside Air Temperatures.....	38
4.1.2	Riparian Air Temperatures	39
4.1.3	Field Air Temperatures.....	42
4.1.4	Minimum Air Temperatures	43
4.2	Water Temperatures	44
4.3	Riparian Mapping	45
4.3.1	Riparian Inventory.....	45
4.3.2	Temperature overlay	46
4.4	Implications for urban planning, stream management and UHI mitigation	47
5.	Conclusions	50
	References.....	51

Abstract

Vegetation and water bodies are being utilized as tools to cool the local environment and combat intense heat events through water evaporation and vegetation evapotranspiration, shading, and modification of air movement. This study analyzes the magnitude, spatial and diurnal variability of cooling experienced in 20 m, 40 m and 80 m wide riparian zones compared to an unvegetated site along South Creek in southwest Sydney, Australia. Air temperature sensors were placed across the width of the buffer extending into adjacent grass fields, measuring at hourly intervals over the summer of 2022-2023. LiDAR data was used along three 5 km reaches to map the riparian zone, buffer width, and riparian cooling using a simple kriging interpolation.

Vegetated buffer zones were 5-7 °C cooler with more consistent daily maximum temperatures and diurnal variation. Buffer width had little impact on the magnitude of cooling, with the 20 m riparian buffer showing the largest temperature reduction likely due to enhance airflow and river cooling, however the cooling effect of larger buffers extended further beyond the riparian canopy while covering a larger total area. These findings help understand how varying buffer widths can be implemented in urban design to combat the urban heat island effect.

1. Introduction, literature review and thesis aims

1.1 Introduction

Urban centers are both vulnerable and highly exposed to the hazard of high temperatures and extreme heat events (IPCC, 2022). For example Greater Sydney, Australia experience this hazard due to a combination of urban heat island (UHI), and a warming climate (Osmond and Sharifi, 2017; Elgendawy et al., 2020).

The first challenge, UHI, is a product of urban development resulting in higher temperatures primarily through replacing natural surfaces with dark absorptive surfaces causing additional solar radiation absorption and surface longwave radiation (Voogt and Oke, 2003; Weng et al., 201; Montazeri et al., 2017; Solcerova et al., 2017; Yu et al., 2020). Other anthropogenic sources of waste-heat include vehicles, buildings (Sun et al., 2018) and industry resulting in hotter conditions when compared to reference areas that lack significant urban development (Oke, 1973). In Sydney this caused urban environments to be 8-15 °C warmer than reference locations over the summer of 2013/14 (Osmond and Sharifi, 2017; Caccetta et al., 2019). Despite coastal winds reducing ambient air temperatures, a multi-year study on Sydney's UHI effect highlighted how the more western suburbs experience higher temperatures as a result of the local climate and UHI (Santamouris et al., 2017). Western Sydney was found to experience triple the number of days over 23 °C than Eastern coastal areas with maximum UHI intensity being nearly twice as high in Western Sydney at 5.1 °C and 5.7 °C than Eastern coastal areas (Santamouris et al., 2017).

The second challenge is climate change related warming, which has resulted in the 2010s and 2020s decades being some of the hottest on record. Significant warming in Sydney in 2019 saw average daily maximum temperatures being 2.2 °C warmer, as well as 19 additional days over 30 °C than the long-term (1961-1990) average (Bureau of Meteorology, 2019). This trend is projected to result in Sydney's 2060 – 2079 climate having 1.6-2.5 °C higher maximum temperatures along with 10 – 20 additional days over 35 °C annually (Office of Environment and Heritage, 2014).

The combination of UHI and climate induced warming presents a significant challenge with extreme heat events becoming more common, intense, and lasting longer (Office of Environment and Heritage, 2014). These events cause significant and varied impacts to anthropogenic and natural systems. In urban environments heatwave events have resulted in infrastructure stress and breakdowns due to power outages and increased demand on healthcare services (McEnvoy et al., 2009; Kjellstrom et al., 2013). Natural systems are also vulnerable to these events with a persistent

heatwave in Western Australia in 2009 resulted in “catastrophic mortality events” in avian species (McKechnie and Wolf, 2010). In other parts of the country future projected warming and changes to rainfall have been predicted to result in several vegetation communities being at risk of extinction (Williams et al., 2003).

Major development has been planned in Western Sydney which already features the hottest summer temperatures, the highest number of extreme heat events as well as an UHI effect of ~ 9 °C (Osmond and Sharifi, 2017; Santamouris et al., 2017; Greater Sydney Commission, 2018a). This is expected to become more severe with regional development creating around 185,000 new homes and the population to grow by nearly 500,000 by 2036 (Greater Sydney Commission, 2018a). As a result, several development plans look at ways to create more “sustainable” and “livable” urban environments (Greater Sydney Commission, 2018a) to address current and future issues of heat. A major component of these plans is the creation and use of additional greenspace for recreation areas as well as to act as thermal refuges, centered around the South Creek and catchment (Greater Sydney Commission, 2018b). This is rare for metropolitan plans with a review of 18 plans for cities around the world found that strategies to address UHI were rarely included, with plans that did consider options to combat UHI lacking evidence-based responses and quantitative data (Elgendawy et al., 2020). This contrasts with many studies globally, exploring the use of urban greening to combat UHI and the cooling impact of vegetated locations (Yu et al., 2020). Vegetated landscapes (greenspace) and aquatic elements (bluespace) have been shown to naturally cool surrounding areas, reducing temperatures via evaporation from water surfaces as well as evapotranspiration and shading from vegetation (Gunawardena and Wells 2017; Yu et al., 2020; Mirabi and Davies, 2022). Rivers and their associated riparian zone offer both these cooling aspects while also providing a diverse array of socio-ecological functions including unique habitat and microenvironments (Booth et al., 2004). These environments can greatly improve and protect river health (Sweeney and Newbold, 2014), with available greenspace also being linked to numerous human health and wellbeing benefits (Frumkin et al., 2017).

Several definitions for the riparian zone exist (Dufour et al., 2019) with this study considering both the definitions proposed by the National Research Council (US), and the NSW Government. The National Research Council (US) considered a variety of interdisciplinary definitions when creating their definition of riparian zones as the channel and streamside zones of rivers and streams that act as *“transitional zones between terrestrial and aquatic ecosystems... distinguished by gradients in biophysical conditions, ecological processes, and biota. They are areas through which surface and*

subsurface hydrology connect water bodies. They include those portions of terrestrial ecosystems that significantly influence exchanges of energy and matter with aquatic ecosystems (i.e., a zone of influence)” (National Research Council, 2002, pg 33). The NSW Government, through the Department of Planning and Environment, classifies the riparian zone based on the physical aspects of the stream environment, with the riparian zone or *vegetated riparian zone* being the vegetated sections either side of a river channel within a *riparian corridor* (Department of Planning and Environment, 2022a). This study considers vegetated and unvegetated riparian zones. Vegetated zones being forested, containing a continuous canopy from river channel to the buffer width extent, while unvegetated zones may contain shrubs and grasses, but do not contain larger trees or shrubs that provide shade. This definition is more in line with the vegetated riparian corridor environment, present in the NSW guidelines (Department of Planning and Environment, 2022a).

This chapter will review environmental benefits of riparian zones, thermal interactions between the river and riparian zone, riparian microclimate conditions, the use of riparian zones to combat UHI, and how remote sensing, geographic information systems (GIS) and modelling has been applied in this context.

1.2 Environmental benefits of riparian zones in urban streams

The presence or absence of riparian vegetation can alter channel morphology (Brierley et al., 1999), water quality, sediment regime (Booth et al., 2004), flood severity (Anderson et al., 2006) and species distributions (Richardson et al. 2005; Sabo et al., 2005). Sweeney and Newbold (2014) reviewed the services and impacts riparian buffers provide. They found that when vegetated and unvegetated rivers are compared riparian vegetation and the presence of a riparian buffer resulted in significantly wider channels in 5th order streams, reduced bank erosion and meandering, increased roughness and debris, and sufficient habitat quality to maintain fish and macro invertebrate communities. Riparian vegetation also has a significant effect on river temperature through shading of the water’s surface (Poole and Berman, 2001; Caissie 2006). River temperature has been used as a critical variable in assessing the health of river systems, particularly when species have temperature tolerance limits at various stages of their life cycle (Kristensen et al., 2014). A review by Balcombe et al. (2011) identified temperature thresholds for several Australian freshwater species like the Murray Cod (*Maccullochella peelii*), Trout Cod (*Maccullochella macquariensis*) and Northern River Blackfish (*Gadopsis marmoratus*) which are expected to

experience declines in populations and distributions due to a combination of increasing temperatures and reduced flows. On the other hand, more temperature resilient species may see an increase in population due to reduced competition and expanded range (Balcombe et al., 2011).

Urban development commonly results in streams and rivers being heavily modified and the removal of large riparian zones. Additionally due to the high surface impermeability of urban areas, stormwater flows and urban runoff is a major source of stream degradation (Palmer et al., 2014). The removal of vegetated riparian zones and replacement with urban surfaces has further worsened this issue, impacting the ecological health of the riparian zone and its ability to provide environmental benefits and ecosystem services (Booth et al., 2004; Newham et al., 2011; Palmer et al., 2014). Booth et al. (2004) have assessed how anthropogenic stressors impact local ecosystems. For example, how anthropogenic disruptions such as land use change, water extraction or pollution can alter the characteristics of the aquatic and terrestrial habitat resulting in flow on effects for species present. Vegetated riparian buffers can counteract and protect many rivers abiotic factors and provide unique microenvironments vital for invertebrates (Rykken et al., 2007b), amphibians (Olson et al., 2007), adding to species richness and biodiversity (Richardson et al. 2005; Sabo et al., 2005). However, some studies have shown that high levels of urban runoff due to impermeable surfaces during storms can bypass the buffer effects of vegetated riparian zones (Walsh. 2004; Walsh et al., 2005). Nevertheless, even limited revegetation efforts has been shown to improve immediate stream conditions despite the surrounding urban environment (Thompson & Parkinson, 2011).

1.3 River Thermodynamics

A prominent feature of the relationship between the riparian zone and its associated water system is its ability to reduce incoming solar radiation to moderate both air and water temperatures, as well as maintain soil moisture (Evans et al., 1998; Caissie 2006; Rykken et al., 2007a; Gunawardena et al., 2017). Surveys and models of the river energy budget find that net solar radiation (short-wave radiation) is the dominant component with net long-wave radiation and evaporative heat flux being less significant factors (Evans et al., 1998; Caissie 2006). Webb and Zhang (1999) found that net radiation accounted for 85% of energy gained and 27% of energy loss. Most of the energy exchange has been found to occur at the air/water interface at 82%, and 15% occurring at the streambed/water interface (Sinokrot and Stefan 1994). Other important factors determining water

temperature include flow variables such as discharge and residence time within a particular reach, as well as the input of water from different sources including tributary streams, precipitation, groundwater contributions, and anthropogenic (Loicq et al., 2018).

There have been ongoing studies to predict and classify water temperature and describe a river's thermal regime. Early attempts categorised thermal regimes based on latitude or on maximum temperature as 'equatorial', 'tropical' or 'temperate' (Smith, 1972). However, these generalizations have largely failed to adequately analyse thermal regimes due to the complex and individual characteristics of each stream and the environmental and climatic conditions within which it is set (Caissie 2006). More local, reach-based variables such as river type and channel orientation are important factors for stream temperature as they dictate the extent to which the channel and associated waters are exposed to solar radiation and the effectiveness of riparian shading (Jackson et al., 2021).

1.4 Riparian Microclimate

What makes a riparian zone unique from other forested areas in the landscape is the edge effect of water bodies that increase local relative humidity and decrease air temperature (Gunawardena et al., 2017). As a result of evaporation, the sensible heat of the air is transferred to the latent heat of the water, reducing local air temperatures, and increasing relative humidity (Gunawardena et al., 2017). Additionally, dense forested riparian zones create microclimates of more moderate temperatures and humid conditions than unvegetated locations, through the processes of evapotranspiration and protection from winds and outside conditions (Syafii et al., 2016). These two forces of river evaporative cooling (river channel effect) and riparian vegetation evapotranspiration and shading (riparian vegetation effect) interact with each other and intruding external temperatures (edge effect) to create and define the riparian microclimate (Figure 1).

Rykken et al (2007a) measured internal microclimate gradients for air and soil temperatures, as well as humidity for headwater streams in Oregon, US. They report a ~ 7 °C increase in afternoon air temperatures within the first 10 m of the river channel at their unvegetated site. The river channel effect extended to 20 m in fully forested environments.

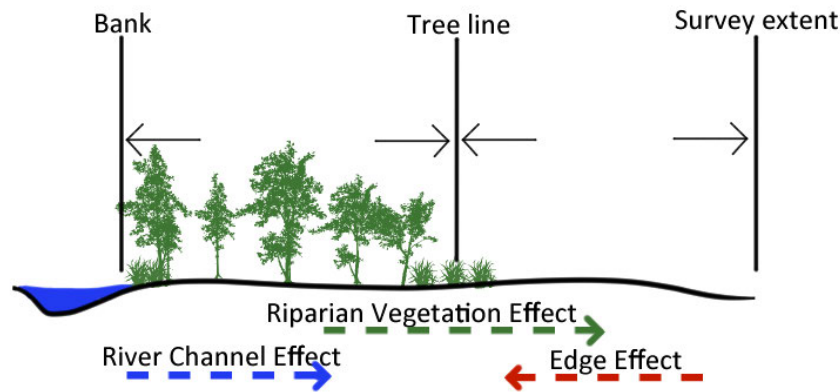


Figure 1: Cooling and warming forces across the riparian zone. Adapted from Rykken et al (2007a).

Du and Song (2016) found that larger water bodies such as lakes exhibited a stronger cooling (river channel) effect than smaller rivers in Shanghai, consistent with Ji and Zhu (2013) who studied rivers ranging from 8 m to 64 m in width. However, the impact of water depth on the riparian microclimate cooling experienced remains unexplored (Liang et al., 2021). Latitude has been found to affect urban blue space with lower latitude cities benefiting from a stronger cooling intensity (Yu et al., 2020). More local environmental factors have a high degree of influence such as prevailing wind (Syafii et al., 2016), and obstructive buildings or geography (Park et al., 2019). Park et al (2019) found wind played a significant role in a small, largely unvegetated waterway in Seoul, with windspeed extending the maximum extent of cooling from ~40 m at 1.15 m/s to ~100 m at 2.03 m/s.

Similar to blue space, green spaces size has been positively correlated with the extent of cooling (Yu et al., 2020) with shape of these spaces influencing total shaded area and ability to promote airflow, determining the cooling extent and strength (Yu et al., 2020). However small and irregularly shaped spaces can have compromised cooling effects when they fail to form a stable internal microclimate (Kong et al., 2014). Additional factors such as vegetation type; grasses vs tree and leaf area index (LAI) have been found to be closely linked. Hardin and Jensen (2007) found that as the value of the LAI doubles, air temperature can drop by 1.2 °C. Hathway et al. (2012) found that the presence a riparian buffer was able to increase the amount of cooling at greater distances from the channel. Rykken et al. (2007) found clearcut forest locations to be significantly drier and hotter in the afternoon compared to locations with a 30 m buffer and fully forested sites. They also identified a 5-6 °C decrease in 3 PM temperatures at the vegetated sites. Similarly, Anderson et al. (2007) found daily maximum temperatures to be 6-9 °C hotter in unvegetated sections of headwater streams in

western Oregon. The Tsai et al. (2017) study in Sheffield, UK found more moderate differences with non-riparian locations being 1 °C warmer and 3 °C warmer in extreme hot weather.

The Yu et al. (2020) review of urban blue and greenspace studies found that landscape composition and other local environmental factors played a major role in the amount of cooling experienced. This resulted in variations between studies in the amount of cooling recorded, differing definitions of UHI, target temperature data, spatial resolution, and background climate factors as other contributing elements.

1.5 Remote sensing and modelling

Temperature and incoming radiation models have been widely employed to quantify the impact of riparian vegetation on water temperatures due to its ability to insulate incoming solar radiation (Greenberg et al., 2012; Loicq et al., 2018; Dugdale et al., 2019; Justice et al., 2020). Other studies have used remote sensing data to produce shade and temperature maps to better analyse the effectiveness of revegetation projects (Justice et al., 2020) or to project the impact of forest harvesting on water temperatures (Greenberg et al., 2012).

Several options for using remotely sensed data are available for identifying riparian vegetation and processing its impact on stream temperature with many studies relying on LiDAR datasets to map and model the riparian vegetation. Dugdale et al. (2019) compares the performance of six distinct vegetation datasets including Structure from airborne Motion photogrammetry (SfM) and a 1 m resolution LiDAR, a 2 m and 5 m resolution Digital Elevation Model (DEM), as well as more geometric polygon layers indicating forested areas. Unsurprisingly the poorer performing models including the lower resolution DEM and polygon layers had a large amount of error when compared to the SfM layer which was used as a reference due to its expected high quality. Estimations for tree height overestimated the height when using lower resolution datasets. LiDAR correlated well with SfM with a slight bias in underestimating tree height (Boyd and Kasper, 2003). These resolution errors can permeate through a model, as Boyd and Kasper (2003) found that inaccuracies in modelled tree height translate to an overestimation in riparian shading and a resulting cooler temperature. When applied along streams, cooler packets of water were further cooled by an overestimation of riparian shade resulting in 1-2°C difference after 2 km.

Greenberg et al. (2012), used a high-resolution LiDAR digital surface model and processed per-pixel shade cast on the water's surface at a given hour to project the removal of the riparian vegetation. They ran the model with, and then excluding the riparian vegetation finding a 9% increase in river solar radiation with vegetation removal with an average 647 Wh/m²/day during summer and a potential 0-15°C water temperature increase (Greenberg et al., 2012). Another study by Wawryniak et al. (2017) calculated shadow factor using a high-resolution DEM and simulated the 3d environment every hour, to model riparian and groundwater associated cooling in a high-order stream in Austria. Including and excluding the impact of shade projected a 10% increase in solar radiation absorbed with temperatures increasing 0.26 ± 0.12 °C and 0.31 ± 0.18 °C for the two modelled periods (Wawryniak et al., 2017). These models can be used to project the impacts of riparian management or channel conditions. Jackson et al. (2021) modelled river channels of varying orientation, width, discharge, and volume, and included obstacles representing riparian vegetation. The difference in incoming radiation was used to determine where the greatest reduction in stream temperatures is along the catchment for existing vegetation and revegetation efforts. Justice et al. (2007) achieved a similar outcome using Heat Source (Boyd and Kasper, 2003), a process-based temperature model which computes effective shade based on channel geometry, orientation, aspect, and vegetation height. The modelled temperature output was compared with 'future' river conditions considering additional vegetation and channel narrowing, highlighting areas for restoration prioritization based on the most effective shading and proximity to known salmon spawning areas.

UHI has been quantified in numerous studies, however microclimate studies for riparian areas are poorly developed (Eskelson et al. 2011) with the Kim and Brown (2021) systematic review of 51 studies measuring and modelling UHI found the majority to focus on the Meso scale (10 -100 km). UHI intensity is the most common target and generally modelled from satellite infrared data to infer land surface temperature (Mather et al., 2017; Sun et al., 2018). Very few studies have attempted to model and map the riparian microclimate regarding the cooling of the surrounding environment. Rocha et al. (2022) mapped the evapotranspiration of urban greenspace around Berlin, Germany based on land use and greenspace location. Using climate conditions and vegetation characteristics they produce large scale heatmaps of evapotranspiration and subdivide this into evapotranspirative cooling service, which is derived from the amount of evapotranspiration (mm/day), and the radiative cooling effects which is the estimated soil temperature cooling due to vegetation shading. Jiang et al. (2020) model differing urban layouts in waterfront districts to identify how greenspace

influences cooling. Their simulations of the 3 urban layouts found that the districts with wider riparian zones resulted in the furthest reaching cooling effect the cooler districts having a buffer width of 90-100 m extending their cooling to 500 to 600 m. Orientation also played a major role with N-S channelling the southerly monsoon cold air leaving it unobstructed (Jiang et al., 2020). Eskelson et al. (2011) created three Kriging derived temperature models of the riparian microclimate considering several variables in addition to distance to stream and vegetation extent. They found that distance to stream and height above stream were the most important covariates with their use of more advance interpolation methods like kriging with external drift, which can incorporate additional covariates and has been more widely used to create microclimate profiles (Eskelson et al., 2011). Other geoprocessing methods for modelling air temperatures between points of know temperature have been widely used in regional scales (Hadi and Tombul, 2018). The different way these models interpolate temperature could result in more accurate models, however Hadi and Tombul (2018) comparison of eight of these spatial interpolation methods including IDW and several Kriging models found no significant difference between methods.

1.6 Thesis Aims and Objectives

Quantitative information on the riparian microclimate and associated cooling is still subject to a large degree of variability and disagreement (Brooks and Snowman, 2009; Yu et al., 2020; Liang et al., 2021). This is largely a product of local and regional factors influencing temperature gradients within the riparian microclimate and altering how cooling is expressed to the surrounding environment (Rykken et al., 2007a). This has resulted in difficulties with firstly, communicating the impact on mitigating extreme heat and secondly, guiding better management practices. Furthermore, few studies have attempted to spatially map the riparian microclimate (Eskelson et al., 2011) and, there is a lack of blue and greenspace studies in the study area of Sydney for the types of local vegetation present. To address these issues this thesis has four aims:

1. To measure air temperature within riparian zones of varying buffer width and adjacent fields.
2. To quantitatively define the impact and extent of the river channel, riparian vegetation, and edge effects, and how these are impacted by differing riparian zones widths.
3. To produce riparian zone heat maps from temperature models using remotely sensed data.

4. With both field-collected and remote-sensed data, classify the most effective riparian buffer width for reducing internal and surrounding temperatures with a focus on combatting urban heat.

Additionally, the thesis hypotheses are:

1. Vegetated areas will have lower daily maximum temperatures than unvegetated areas, due to the presence of riparian vegetation cooling.
2. Internal daily maximum temperatures of the vegetated riparian zones will decrease with increasing width, due to stronger riparian vegetation cooling.
3. Riparian vegetation cooling at sites with larger buffer widths will extend further into the adjacent fields.

Addressing these aims will help inform river management practices and urban designers on how to create effective riparian microclimates and utilize the cooling potential of these zones to combat extreme heat.

2 Regional Settings and methods

2.1 Regional Setting

South Creek is a tributary stream of the Hawksbury River and the truck stream of the Wianamatta South Creek Catchment. Southwest Sydney sees maximum temperatures range from 30.2 °C in January to 17.5 °C in July with an annual mean of 24 °C (Bureau of Meteorology, 2023b). Peak temperatures were recorded January 2020 at 47.6 °C. On average there are 55.3 days over 30 °C a year. Solar exposure is highest over December with mean daily exposure at 6.27 kWh/m²/day estimated from satellite imagery (Bureau of Meteorology, 2023b). Total yearly discharge for South Creek has ranged from the lowest in 1994 at 1,093 ML/year to the highest in 2022 at 313,335 ML/year (Bureau of Meteorology, 2023a) with a mean annual rainfall of 716 mm (Bureau of Meteorology, 2023b). Typically, peak flows occur during March, however median monthly flows are similar across February, March, June, July, and December and range from 0.29 to 0.076 m³/s (Bureau of Meteorology, 2023a).

South Creek is 5th order stream based on the Strahler classification until it's confluence with Thompsons Creek at the Rossmore marking (Figure 2B) where it becomes a 6th order stream. The 63

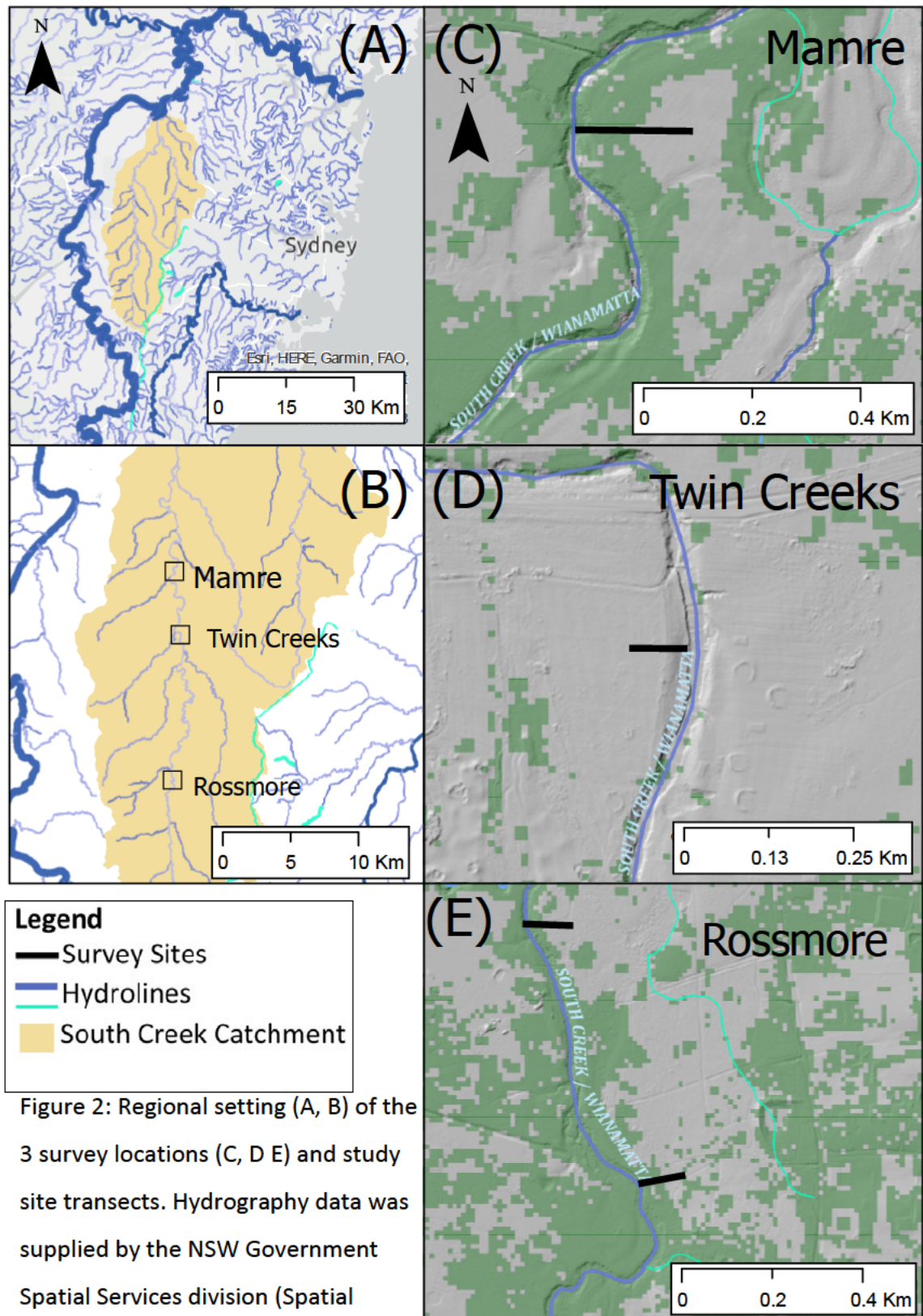
km length descends 90 m in elevation from its origin at Orland Park, with the catchment covering a total area of 617 km². South Creek runs through a mix of suburban and agricultural lands resulting in a mix of unforested grazing lands and sections of remnant vegetation. Based on the NSW Department of Planning and Environment riparian guidelines, riparian zones (or vegetated riparian corridors) are to extend 40 m either side of the channel (Department of Planning and Environment, 2022a). As a result of a history of land clearing and more recent urban development South Creek is considered one of the most degraded catchments along the Hawkesbury-Nepean River system (Department of Planning and Environment, 2022b). Several public parks and reserves are situated along the river resulting in some instances of a larger intact Cumberland Riverflat Forest which includes canopies of rough-barked apple (*Angophora floribunda*), broad-leaved apple (*Angophora subvelutina*) with sections of forest red gum (*Eucalyptus tereticornis*) and cabbage gum (*Eucalyptus amplifolia*) (Benson and Jocelyn, 1990). The understories are populated with a cover of grasses with small herbs and ferns. Adjacent areas or sections featuring no riparian zone contain t Tussock and Rytidosperma grasses, with grazing sites featuring shorter Paspalum grasses (Benson and Howell, 1990).

2.2 Site characteristics

Along the trunk stream of South Creek, four sites were selected to represent differing riparian buffer widths. These include the largely unvegetated site at the Twin Creeks location with a 0 m wide riparian buffer, medium and well vegetated sites at the Rossmore location representing 20 and 40 m buffer widths and a highly vegetated site at the Mamre location with an 80 m buffer width (Figure 2). Specific measurements and sensor placement in each zone are highlighted in Figure 6.

Selection criteria for determining site included morphological attributes of the river and surrounding floodplains with each site requiring similar characteristics including a channel North – South orientation, lack of tributary inclusions, similar channel width and depth, as well as similar vegetation community while being easily accessible with landowner permission. Additionally, the vegetated sites needed a continuous forested riparian zone which bordered unvegetated grasslands. Riparian zone width was first measured with ESRI world imagery (available at https://services.arcgisonline.com/ArcGIS/rest/services/World_Imagery/MapServer) using measurement tools in Arc GIS Pro 2023 as part of the Macquarie University licensed software (Environmental Systems Research Institute (ESRI). (2023). ArcGIS Release 3.1.0 Redlands, CA, USA)

based on the trees bordering the river and the edge of the riparian zone and then at each site with transect tape. Ideally riparian buffer width was consistent on both channel sides and along the river channel for at least 50 m up and downstream of the transect.



Mamre: The Mamre site is located along a heavily vegetated section of South Creek featuring riparian forests extending ~40 – 80 m from the river channel. This is due to the Samuel Marsden Reserve and sports field, and the heritage listed Mamre Homestead present on either side of the river. Vegetation at this site features an intact Cumberland Riverflat Forest with a dense eucalypt canopy leading to a fenced off grazing field with *Paspalum* grasses (Figure 3). In 2000 the site was subject to a regeneration program that expanded the width of the riparian buffer zone from ~40 m to ~80 m where Cabbage Gum (*Eucalyptus amplifolia*), Rough-barked Apple (*Angophora floribunda*) and Swamp Oak (*Casuarina glauca*) seedlings were planted (Department of Environment and Conservation, 2005). Additional weeding and the removal of invasive mid-storey species was also conducted. The river channel is ~10 m wide and has steep ~2 m high banks.



Figure 3: Mamre site at the river channel (A) right bank looking downstream and at the riparian edge (B).

Rossmore: The Rossmore sites feature a smaller riparian buffer of ~20-40 m along the Rossmore Grange Nature Reserve and rural domestic properties (residential and farm infrastructure (Department of Planning and Environment, 2020). The riparian corridor is primarily vegetated with Swamp Oak (*Casuarina glauca*) with sections of Cabbage Gum (*Eucalyptus amplifolia*). The surrounding fields are dominated by Tussock and *Rytidosperma* grasses (Figure 4). Several shrubs and backswamps are present in the extending parkland visible in the vegetation map (Figure 2). The river channel is narrower, ranging from ~5-7 m across and flat, rising less than 0.5 m. The 20 m and



Figure 4: Rossmore site at the river channel (A) right bank looking downstream and at the riparian edge (B).

40 m sites feature very similar channel and floodplain characteristics except for a 3 m wide fire-trail path that intersects riparian canopy at the 20 m and 30 m sensors at the 40 m site.

Twin Creeks: The Twin Creeks site features a dense mix of ~1-1.5 m high *Rytidosperma* grasses, mainly Wallaby grass (*Rytidosperma Caespitum*). Several 1-2 m high Lantana shrubs populate the grassland. Scattered Swamp Oaks populate the eastern side of the river channel which ranged from ~10-15 m wide with steep 3 m banks on either side (Figure 5).



Figure 5: Twin Creeks site at the river channel (A) right bank looking downstream and at the (left bank) channel edge looking away from the river (B).

2.3 Methodology

2.3.1 Sensor Placement

At each study site a temperature sensor array was installed along the riparian zone on the West side of the river channel for the vegetated 20 m, 40 m and 80 m sites, and the East side for the unvegetated zone due to other sites being unavailable. Sensors along the arrays were spaced 10 m moving perpendicular from the river channel as displayed in Figure 6. Additional sensors were placed at 5 m from river channel and riparian edge.

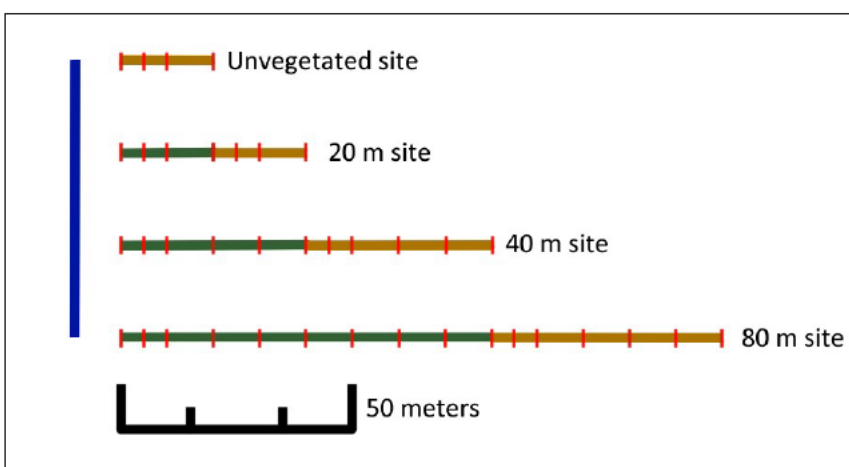


Figure 6: Sensor placement at each study site. Sensor location is indicated with red tick along the riparian zone (green) and adjacent field (yellow), moving away from the river channel (blue).

iButton DS1925 (Maxim/Dallas Semiconductor Corp., USA) temperature sensors were installed 1 m above the ground facing west and attached to wooden stakes or trees where available, an example of the wooden stakes with sun shield can be seen in Figures 3B, 4B and 7. The sensors were fixed to rubber based adhesive tape which was then nailed to the stakes or trunks to avoid a direct sensor to tree or stake connection. Aluminium flashing sheets were placed above each sensor to block any direct sunlight. Sensors were missioned to record hourly, on the hour, at an accuracy of 0.0625 °C. Additionally, two HOBO MX2201 (Onset, Bourne, MA, USA) temperature sensors with an accuracy of (0.5 °C) were installed instream at the beginning of each sensor array on the water surface and channel bed. The water temperature sensors were also missioned to record temperature hourly, on the hour. Both air and water temperature sensors collecting data between the 29th of November 2022 to the 6th of March 2023 across all sites. Each of the water and air temperature sensor were tested together before and after installation to record any deviation between each sensor.

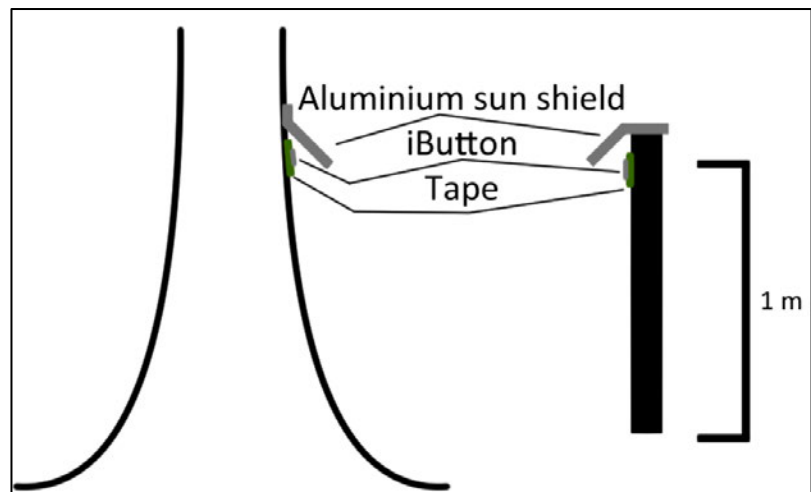


Figure 7: Sensor fixture to tree trunks (left) and wooden stakes (right)

2.3.2 Data processing

Sensor data was classified between each site and zone including water, riparian and field. For both air and water temperatures, daily minimum and maximum values were used to create mean daily maximum and minimum values for each sensor, and hour.

South Creek experienced overbank flooding during the recording period. Therefore, potential outliers were identified if the air temperature daily maximum values for individual sensors were 5 °C lower than the reference weather station data at Badgerys Creek (Bureau of Meteorology, 2023b). This was to avoid analysing air temperatures that were artificially cooler due to being submerged during these flooded, with some sensors at the 20 and 40 m sites showed signs of being inundated. The sensors at 20 m at the 20 m site and 85 m at the 80 m site were incomplete from

19th December 2022. To adjust, these daily maximum and minimum values were approximated using the median of the adjacent sensors. The 40 m sensor at the 0 m site had its sun shield folded and covered in mud and vegetation debris likely causing the decrease in maximum daily temperatures observed. As a result, this sensor is ignored in data processing and analysis. Only the channel bed water temperature sensor data was used due to surface sensors repeatedly being exposed to the air due to changes in water level. Furthermore, data between 12th December 2022 and 21st December 2022 was removed due to the 20 m and 40 m channel bed sensors being exposed.

Air temperature sensors were grouped as either riparian or field, based on their zone relative to the 'last tree', or riparian edge sensor being included in both zones. Minitab Statistical software v21.4 (Minitab, LLC, 2023) One-Way ANOVA tests were used assuming equal variances, with Fisher Pairwise comparisons used to compare the unvegetated site with other vegetated sites. This was done for both mean minimum and maximum daily temperatures for riparian and field zone. Differences in the means were considered significant with a P value of < 0.05 . To test for significance between buffer widths the same approach was used to compare vegetated 20 m, 40 m, and 80 m sites for both field and riparian zone. Water and air temperature variation for both mean daily minimum and maximum temperature was also carried out using an ANOVA test for equal variances.

To remove any bias as a result of differing buffer width, common distances were also compared based on sensor temperatures limited to within 20 m of the channel or riparian edge. The same ANOVA tests were conducted on these new riparian and field datasets for each site.

2.3.3 Geoprocessing

To analyse the riparian conditions along sections of South Creek, three 5 km reaches were selected corresponding with our three study locations at Mamre, Twin Creeks and Rossmore as shown in Figure 2B. The placement of the 5 km reach was based on their inclusion of the sensor transects and to avoid tributaries. Geoprocessing was conducted using ArcGis Pro (v3.1.0).

Riparian Inventory: To map riparian width and location along each study reach a riparian inventory map was created highlighting areas of mean riparian vegetation height over 5 m. This map created a Relative Elevation Mode (REM) of each reach based on a LAS formatted LiDAR downloaded from the Elevation and Depth - Foundation Spatial Data (ELVIS) portal, (<https://elevation.fsdf.org.au/>)

that was collected on 16th July 2019 with a 0.3 m vertical and 0.8 m horizontal accuracy and 4 points per m² density. A section of these REM for each reach is visible in figure 8. The constructed REM was based off the 'first of many' return values with areas including buildings, bridges and powerlines excluded. Output values were limited to 0 – 10 m in elevation within 80 m of the river thalweg which was manually placed. Mean elevation was calculated over irregular grids extending 500 m along the river and 20 m into the riparian zone with 4 grids on each side of the river to extend to a total of 80 m either side of the river channel. Additionally, a secondary mean vegetation height was calculated for the more immediate river conditions based on 500 x 15 m irregular grids which extended only 15 m either side of the river thalweg. Using mean vegetation height grids with a height over 5 m were classified as 'riparian' allowing for riparian buffer width to be calculated in 20 m intervals. Each 500 m segment had its buffer width classified by the lowest values on either side of the channel.

Temperature Overlay: The temperature overlay map was created for the Mamre and Rossmore locations, along the same 5 km reaches as the riparian inventory maps using the riparian inventory maps to determine riparian extent (Figure 19B, C). An additional map was created for the Mamre reach to simulate unvegetated conditions. Temperature points were placed at the channel, riparian edge, and survey extent every 50 m. The values of these points were based off mean daily maximum values collected at the air temperature sensors arrays. As the magnitude of cooling varied little between the different buffer widths (Figure 11) values for the vegetated sections were kept consistent at 26.5 °C for bank locations, 27.8 °C at the riparian edge and 35 °C at the survey extent. The unvegetated sections had bank temperature points of 30.8 °C and 35 °C at the survey extent. An additional line of points 5 m beyond the channel of 34 °C to represent the extent of the river channel effect. Ordinary Kriging using a Spherical semi-variogram model with each cell considering the values of 20 temperature points. IDW processing was tested as an alternative however performed poorly resulting in maps overexpressing the individual temperature points rather than the differing zones. The variable search radius set to 20 points considered produced the clearest maps with the option of set distance resulting in a poorer projection likely due to the differences between temperature zones (river, riparian edge and survey extent) varying along the target reach. The output raster was limited to a cell size of 5 m² for reduced processing time. A One-way ANOVA not assuming equal variances was used to determine significance between the vegetated and unvegetated Mamre models. Modelled temperatures were calculated along the same 20 m, 40 m and 80 m temperature transects as used in the field (Figure 2).

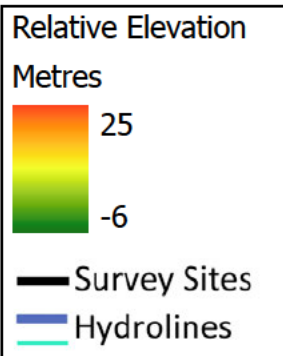
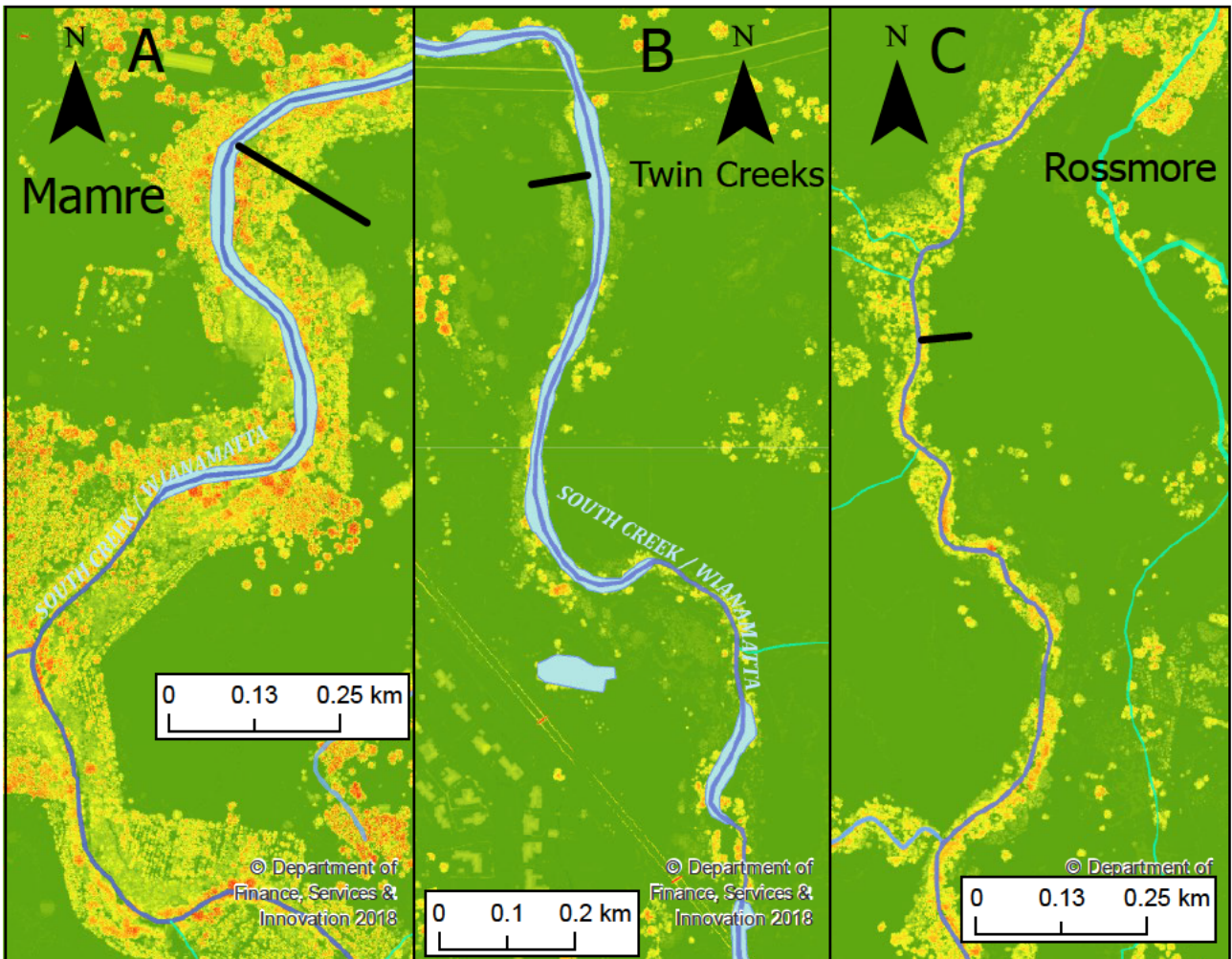


Figure 8: REM model for each study location of Mamre (A), Twin Creeks (B) and Rossmore (C), focusing on areas around each of the study sites.

3 Results

3.1 Riparian Microclimate

3.1.1 Daily maximum and minimum air temperatures

Air temperatures were collected between the 29th of November to the 6th of March with daily maximum and minimum temperatures for the riparian zones displayed on (Figure 9A) and field temperatures on (Figure 9B). Additionally, correlating daily maximum temperatures from Badgerys Creek weather station are included (Bureau of Meteorology, 2023b). The highest temperatures were recorded at the unvegetated (0 m) site on the 11/02/23 at 44.3 °C. This differed from the vegetated sites (20 m, 40 m and 80 m) that recorded maximum riparian air temperature on the 06/03/23 on the same day as the highest recorded at the Badgerys Creek weather station at 42.2 °C. Maximum field temperatures for the 20 m and 40 m site were also recorded on the 06/03/23 with the 80 m site experiencing its maximum temperature on the 11/02/23 along with the unvegetated site.

Zone	Site	Daily Maximum			Daily Minimum		
		Mean (°C)	StDev	Interquartile Range (°C)	Mean (°C)	StDev	Interquartile Range (°C)
Riparian	20 m	26.61**	4.29*	23.1-29.9	15.56*	2.91*	13.8-17.7
	40 m	28.14*	4.81**	24.3-31.7	15.27*	3.08*	13.6-17.4
	80 m	26.98**	4.06*	24.1-29.8	17.42**	2.63**	15.6-19.6
Field	0 m	33.91	6.096	29.6-38.5	13.875	3.509	11.7-16.6
	20 m	30.32**	5.347*	26.6-34.3	14.06	3.421	11.9-16.5
	40 m	31.85*	5.393*	27.9-36.1	13.65	3.471	11.6-16.1
	80 m	31.94	5.99	27.5-36.2	15.24*	3.331	13.3-17.6

Table 1: Air temperature statistics for riparian and field zones for each site. Asterisks represent significant difference ($P < 0.05$) groupings between sites of varying buffer width. Riparian zones are compared with the 0 m field measurements.

Minimum air temperatures showed less variation in magnitude between each site and weather station data however each site reached their lowest recorded temperature at differing times for both the riparian and field zones. The unvegetated site once again having the more extreme temperatures at 4.1 °C on the 15/12/22 (Figure 9). Compared to the unvegetated site, riparian mean daily maximum temperatures ranged from 7.3°C cooler at the 20 m site to 6.9 °C at the 80 m site, with the 40 m site being the warmest at 5.8 °C cooler (Table 1). The riparian zones were also significantly ($P = 0.00$) less variable with more consistent daily maximum temperatures and significantly ($P = 0.00$) lower standard deviation than the unvegetated site.

Buffer width had a mixed impact on the reduction in daily maximum riparian temperatures (Figure 10). Comparing between the riparian buffer widths, the 40 m site was found to have a significantly ($P = 0.00$) warmer daily maximum riparian temperature of 28.1 °C (Table 1), with temperatures of the 20 and 80 m buffers not being statistically different ($P = 0.205$) despite the large size difference. Furthermore, temperature variation between the 20 m and 80 m riparian zones did not differ significantly ($P = 0.09$), with only the 40 m site showing significantly ($P = 0.00$) lower variation.

The field zones adjacent to the riparian zones each had significantly cooler ($P = 0.00$) daily maximum temperatures than the unvegetated site. The 20 m site experienced the largest reduction in mean daily maximum field temperature of 3.6 °C. The 40 and 80 m sites were cooler to a smaller extent at 2.1 °C and 1.98 °C respectively. The 20 and 40 m sites also experience significantly ($P = 0.00$) less field temperature variation with the 80 m and unvegetated sites having a statistically similar temperature variation ($P = 0.602$).

Analysis of buffer width and maximum field temperatures found that the 20 m site had significantly ($P = 0.00$) lower temperatures compared to the 40 and 80 m sites which were not significantly different from each other ($P = 0.794$).

In contrast, the presence of a riparian buffer saw higher daily minimum temperatures at the vegetated sites compared to the unvegetated site. Mean minimum temperatures within the riparian zones were significantly warmer ($P = 0.00$) compared to the unvegetated site. For the 80 m site, the mean daily minimum temperature was 3.5 °C warmer, 1.4 °C at the 40 m, and 1.7 °C at the 20 m site (Table 1). These riparian minimum temperatures had significantly ($P = 0.00$) less variation.

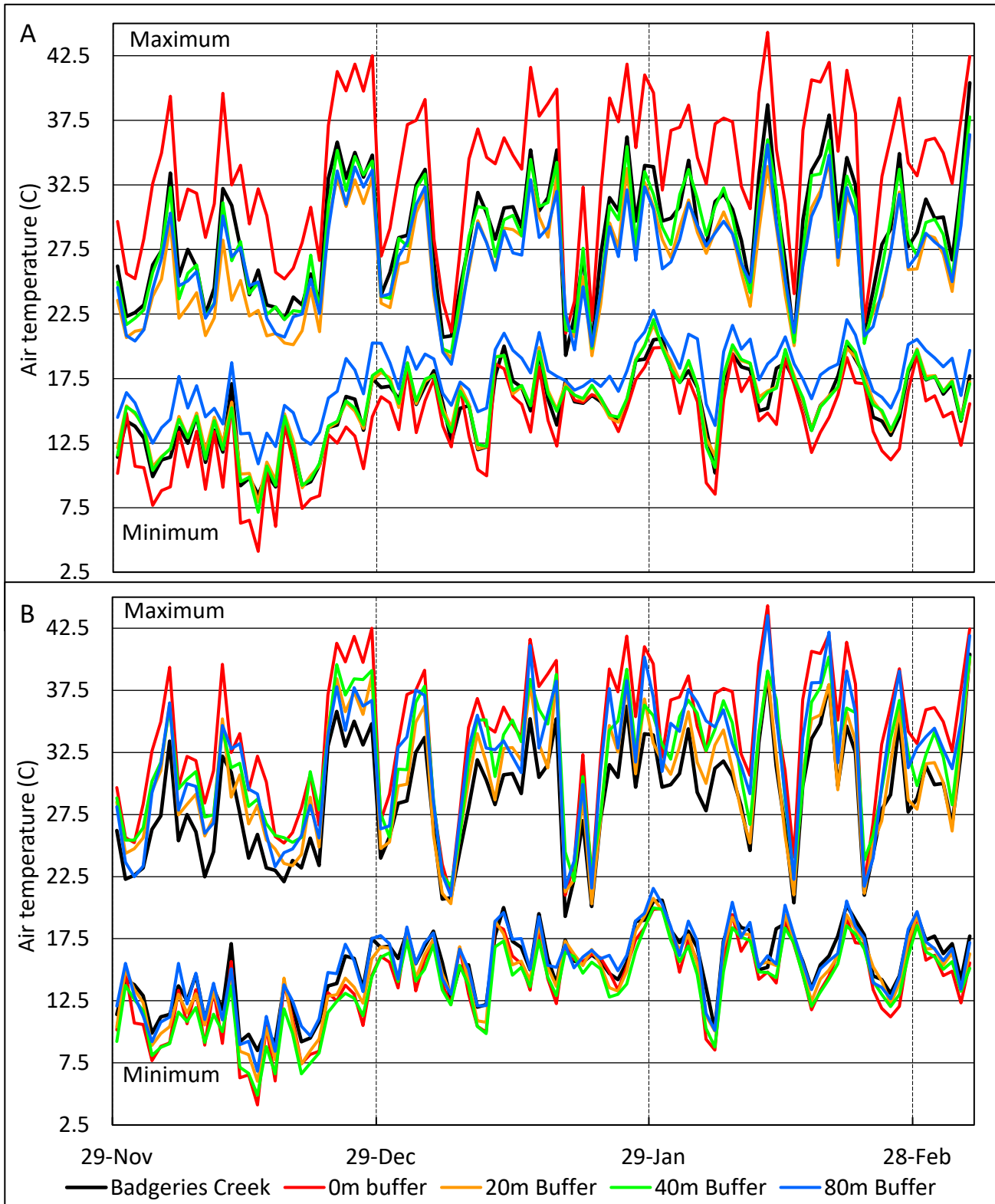


Figure 9: Maximum and minimum daily temperatures across each of the sites for the riparian zone (A) and field (B). Daily maximum and minimum data from the Bureau of Meteorology's Badgeries Creek weather station is also included.

Field minimum daily temperatures varied less between the vegetated and unvegetated sites with the 20 m and 40 m field mean temperatures not being significantly (20 m $P = 0.420$) (40 m $P = 0.259$) warmer or cooler than the unvegetated site, respectively. Only the 80 m site had a significantly ($P = 0.00$) different mean minimum daily temperature being 1.4 °C warmer than the unvegetated site.

Comparing minimum temperatures between the vegetated sites, the 80 m site's riparian minimum temperature is significantly ($P = 0.00$) warmer than the 20 m and 40 m sites which were not significantly different ($P = 0.144$). This was also seen in the field temperatures for each site, with the 80 m site being significantly ($P = 0.00$) warmer when compared to the other 20 m and 40 m vegetated sites which were statistically similar ($P = 0.065$).

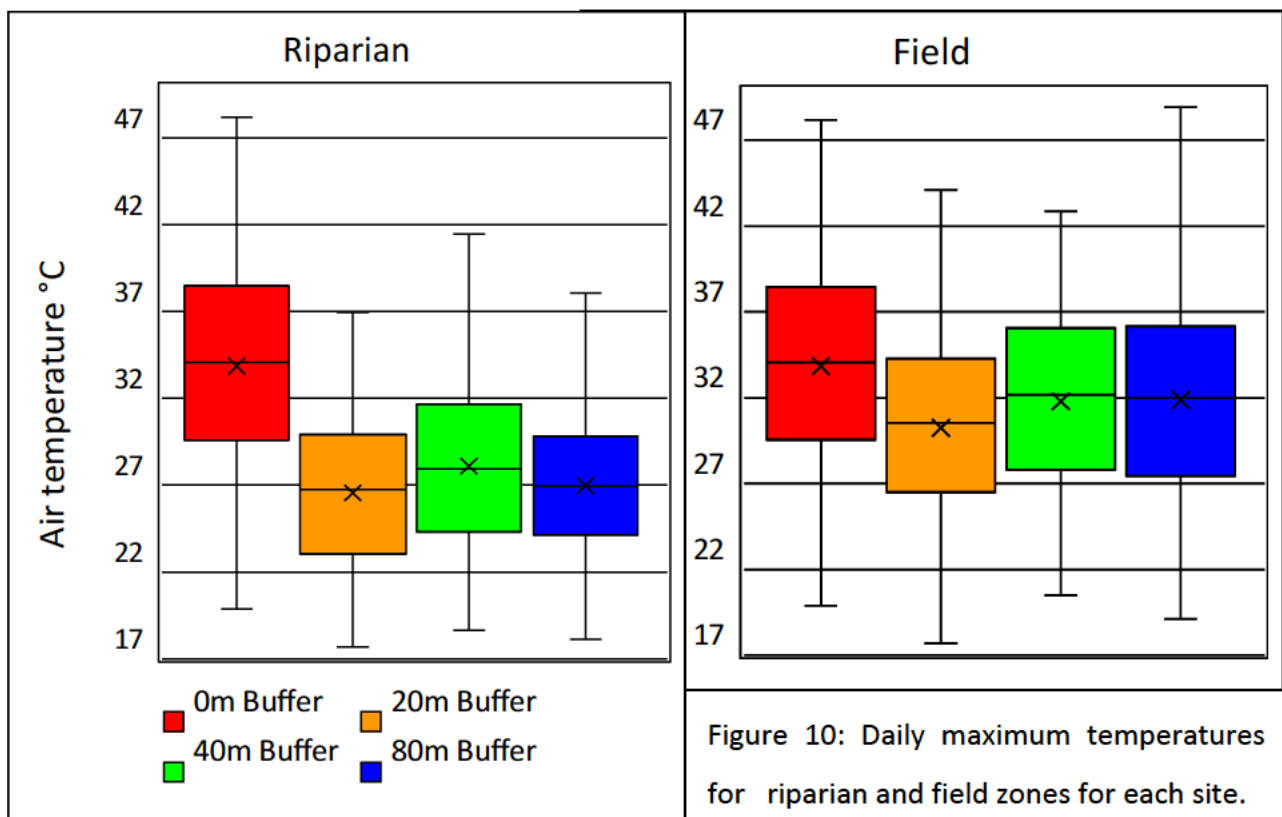


Figure 10: Daily maximum temperatures for riparian and field zones for each site.

X indicates the mean, the middle line indicates median, the whiskers extend to the maximum and minimum.

3.1.2 Air temperature gradients

Across each of the sites maximum air temperatures increased the further from the river channel and the boundaries of each riparian zone. In the unvegetated site, temperature gradients are limited to within 5 m of the river channel with an initial increase of 5.2 °C and then plateauing at ~35 °C for the remaining 35 m. In the vegetated sites, riparian temperature gradients of between 1-2 °C being limited to 10 m at the 40 m site and extending 20 m at the 80 m site, with the 20 m site having no clear temperature gradients within the riparian zone. The wider buffers experienced smoother temperature gradients across the entire riparian zone with the 40 m riparian zone forming a 20 m plateau at 27.9 °C and the larger 80 m zone containing a 40 m plateau at 26.9 °C.

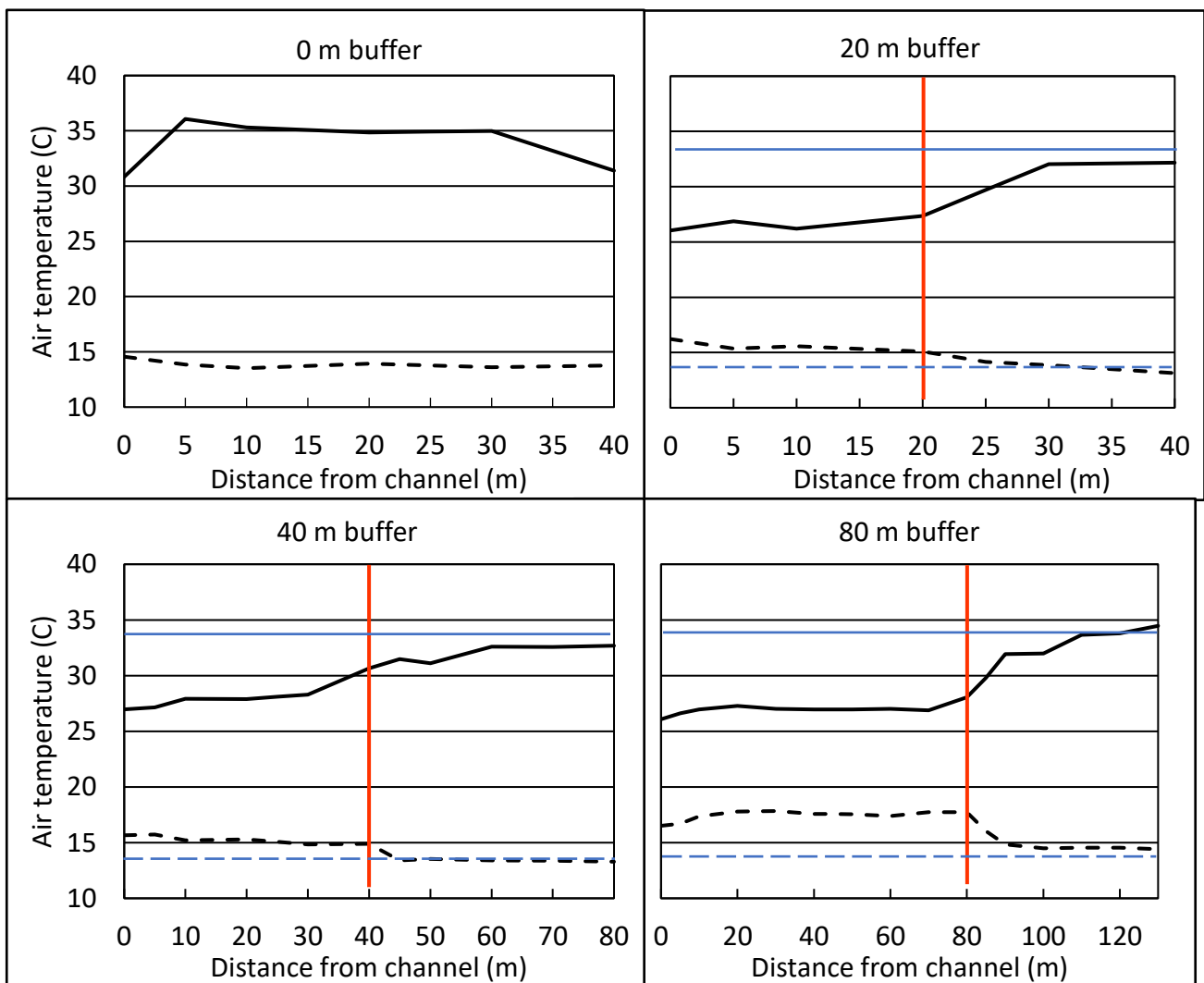


Figure 11: Mean daily maximum (solid lines) and minimum (dashed lines) temperature gradients for each sensor at each site. Mean temperatures for the 0 m site are included for each other site in blue. The red lines indicate the riparian tree line.

The temperature gradients for the 40 m site revealed no clear impact of the ~3 m break in the riparian canopy with temperatures consistent along the 20 – 30 m mark (Figure 11). This trend of smoother temperature gradients extended into the adjacent fields with the 20 m site increasing to plateau after 10 m while at the 40 m site temperatures took 20 m to plateau. The 80 m temperatures increasing rapidly along the 50 m stretch of field surveyed forming no clear temperature plateau.

When examining minimum daily temperature, gradients were flatter compared to maximum temperatures with the unvegetated site experiencing a $-0.78\text{ }^{\circ}\text{C}$ shift in temperature across the 40 m survey area, with the majority of this trend occurring within 10 m on the river channel. The vegetated zones also had a small temperature shifts within 5 m of the stream channel with temperatures decreasing $1.25\text{ }^{\circ}\text{C}$ at the 20 m site within 5 m of the channel while the 40 m site steadily decreased $0.9\text{ }^{\circ}\text{C}$ within 10 m of the channel. The larger 80 m riparian zone was found to increase minimum temperatures moving into away from the channels edge followed by a steep $2.8\text{ }^{\circ}\text{C}$ decrease moving 10 m beyond the riparian zone. This temperature reduction as also present to a lesser degree at the 40 m site with temperatures decreasing $1.5\text{ }^{\circ}\text{C}$ 5 m beyond the riparian zone.

3.1.3 Common distance air temperatures

When comparing the daily maximum air temperatures at common distances for each site and zone to account for the larger areas surveyed for the 40 m and 80 m sites, the impact of buffer width is minimal with the 20 m riparian zone still significantly cooler ($P = 0.00$) (Table 2). However, the 40 m is $0.6\text{ }^{\circ}\text{C}$ cooler when limiting the selection of sensors to 20 m. Field temperatures are also lower by $0.39\text{ }^{\circ}\text{C}$ and $1\text{ }^{\circ}\text{C}$ for the 40 and 80 m respectively. Despite this decrease the 20 m field daily maximum temperatures were still significantly ($P = 0.00$) cooler than the 40 and 80 m, however the 80 m was now significantly cooler than the 40 m zone ($P = 0.00$). Linear temperature gradients across the vegetated sites highlight similar rates of increase ($0.25\text{ }^{\circ}\text{C}/\text{m}$) in the first 20 m of the riparian zone (Figure 12A), with the 40 m site starting with a $0.8\text{ }^{\circ}\text{C}$ higher bankside temperature. Beyond the riparian zone the 20 m site increases the fastest at $1.6\text{ }^{\circ}\text{C}/\text{m}$ followed by the 80 m site at $1.4\text{ }^{\circ}\text{C}/\text{m}$ with the 40 m site gaining temperature the slowest $0.4\text{ }^{\circ}\text{C}/\text{m}$ (Figure 12B).

Table 2: Air temperature statistics for the first 20 m of the riparian and field zones for each site. Asterisks represent significant difference ($P < 0.05$) groupings between sites of varying buffer width. Riparian zones are compared with the 0 m field measurements.

Zone	Site	Mean (°C)	StDev	Interquartile Range (°C)
Riparian	20m	26.62**	0.611	26.08-27.24
	40m	27.48*	0.495	27.01-27.90
	80m	26.729*	0.509	26.21-27.19
Field	0m	33.908	2.209	31.26-35.49
	20m	30.32	2.27	27.95-32.14
	40m	31.461	0.824	30.77-32.31
	80m	30.88	2.46	28.49-33.24

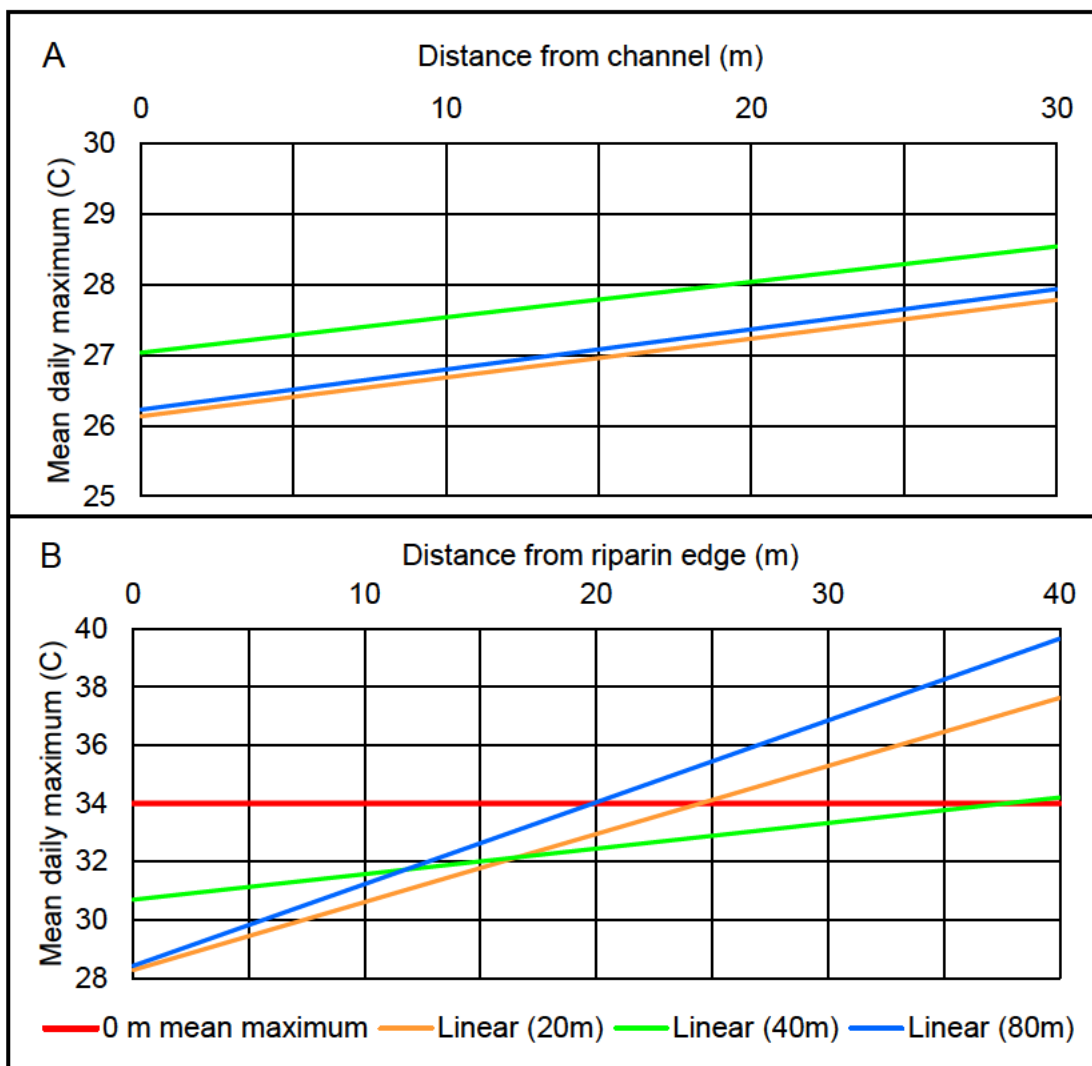


Figure 12: Linear temperature gradients for the first 20 m of the riparian zone (A) and field (B).

3.1.3 Diurnal air temperature variation

When comparing the vegetated and unvegetated sites, the riparian microclimate experiences smoother temperature gradients and mixed peak temperature times (Figure 13A). The most pronounced difference occurs when examining mean hourly maximum temperatures, with the unvegetated 0 m site reaching its daily maximum later in the day at higher temperatures (44.3 °C at 4 PM). In contrast the riparian temperatures were lower by 10.2 °C at the 20 m riparian zone and 8.1 °C at the 40 m and 80 m zone. The riparian zones also reached maximum daily temperatures earlier in the day at 2 PM at the 20 m and 40 m site, while at the 80 m site maximum temperature plateaued, changing only 0.54 °C between 2 and 4 PM.

Overnight temperature gradients were also more moderate in the riparian zones with the unvegetated site decreasing rapidly after 6 PM to become colder than the riparian zones by 9 PM. Similarly in the morning the unvegetated site changed from coldest to hottest, increasing by 9.9 °C from 6 AM to 9 AM.

Minimum hourly temperatures were less impacted by the presence of a vegetated riparian zone, with 8 AM – 8 PM

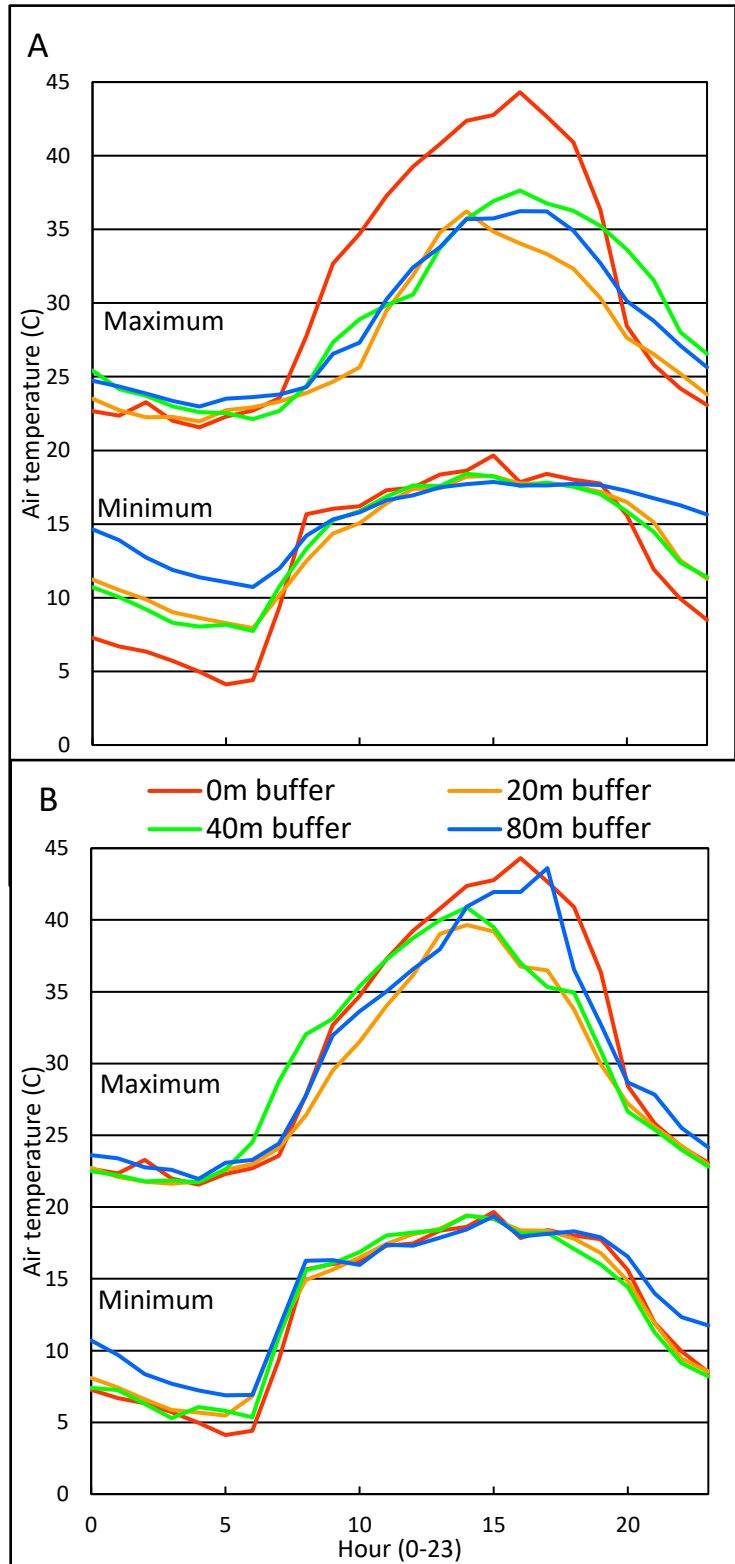


Figure 13: Mean riparian (A) and field (B) maximum and minimum hourly temperatures for each site.

The 0 m unvegetated site is included in both riparian and field datasets.

temperatures being similar across all sites (Figure 13A). However, overnight the vegetated riparian zones were 5 – 10 °C warmer with the larger 80 m riparian zone creating the warmest overnight temperatures.

Maximum hourly field temperatures at the vegetated sites experienced cooler temperatures during the day, with the 20 m and 40 m field temperatures between 12 and 6 PM being significantly ($P = 0.00$) cooler than the 0 m site (Figure 13B). The 80 m field was not ($P = 0.149$). Similarly, to the riparian zones the daily maximum field temperatures arrived earlier for the 20 m and 40 m sites at 2 PM. The 80 m site peaked later in the day at 5 PM reaching 43.6 °C, surpassing the unvegetated site before rapidly cooling in the following hours. Minimum hourly field temperatures followed showed a similar but less pronounced trend to the riparian temperatures with 8 AM – 8 PM temperatures being similar across all sites (Figure 13B). Minimum hourly values were significantly ($P = 0.00$) higher for the 80 m riparian zone overnight between 8 PM to 8 AM compared to the unvegetated site as well as the 20 m and 40 m sites which were not significantly ($P = 0.00$) different from each other. This 8 PM to 8 AM warming present in the 80 m riparian zone was also present in overnight minimum field temperature being 1.8 °C warmer than the 20 m site, 2.0 °C compared to the 40 m site, and 2.3 °C to the unvegetated 0 m site.

3.2 Water Temperatures

3.2.1 Daily maximum and minimum water temperatures

Across the survey period both maximum and minimum daily water temperatures across each site rose steadily. However, the timing and magnitude of the maximum and minimum temperatures varied, with the unvegetated site reaching its maximum of 27.8 °C on the 21/02/23 and the 80 m site reaching 26.6 °C on the 28/01/23. The 20 m and 40 m sites each reached their maximum water temperature on the 03/02/23 at 25.2 °C and 24.9 °C respectively (Figure 14A).

For minimum daily water temperatures each all sites recorded their minimum temperature on the 21/12/22 of 19.9 °C, 16.56 °C, 15.57 °C, and 18.32 °C for the unvegetated, 20 m, 40 m, and 80 m sites respectively (Figure 14B).

Table 3: Water temperature statistics for each site. Asterisks represent significant difference ($P < 0.05$) groupings between sites of varying buffer width. Riparian zones are compared with the 0 m field measurements.

Site	Daily Maximum			Daily Minimum		
	Mean (°C)	StDev	Interquartile Range (°C)	Mean (°C)	StDev	Interquartile Range (°C)
0 m	24.31	1.77	23.1 - 25.6	22.82	1.588	21.7 - 24.1
20 m	22.20*	1.599	20.9 - 23.4	20.72*	1.635	19.5 - 21.9
40 m	21.96*	1.542	21.1 - 23.0	20.45*	1.726	19.2 - 21.6
80 m	23.78*	1.537	22.7 - 25.0	22.31*	1.637	21.2 - 23.6

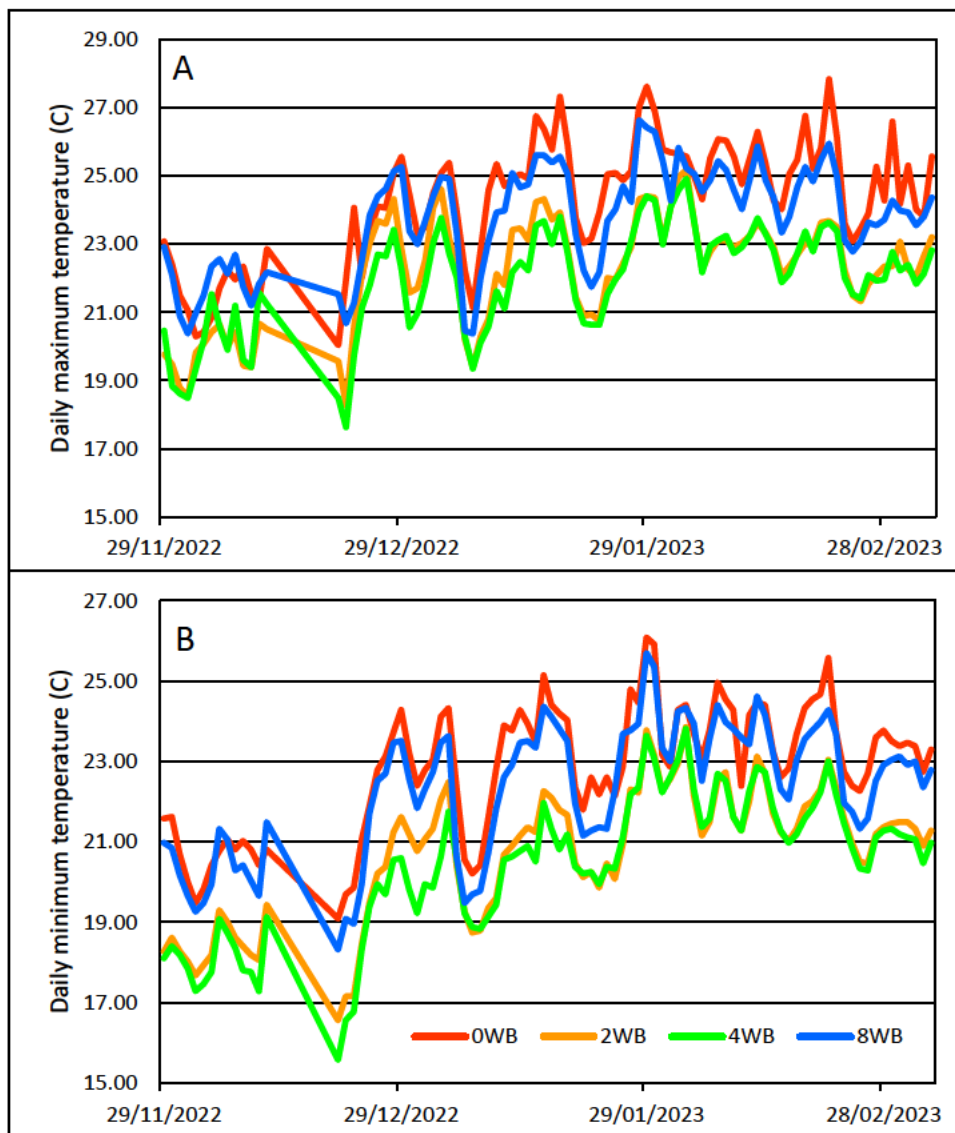


Figure 14: Maximum (A) and minimum (B) daily water temperatures across each of the sites.

Water temperatures also varied between sites, with each of the vegetated sites showing significantly ($P = 0.00$) cooler daily maximum and minimum temperatures than the unvegetated site (Figure 16A). Daily maximum temperatures were 0.5 °C cooler at the 80 m site compared to the unvegetated site, while the 20 m and 40 m site were a further 2.1 °C and 2.4 °C cooler respectively (Table 3). This trend was also maintained for daily minimum temperatures with the difference in maximum and minimum being 2.0 °C (Figure 16B, Table 3). Furthermore, differences in mean minimum temperature mirrored the maximum values. Variation in maximum and minimum daily temperatures did not significantly (daily max $P = 0.467$) (daily min $P = 0.839$) differ between each of the vegetated sites and the unvegetated site.

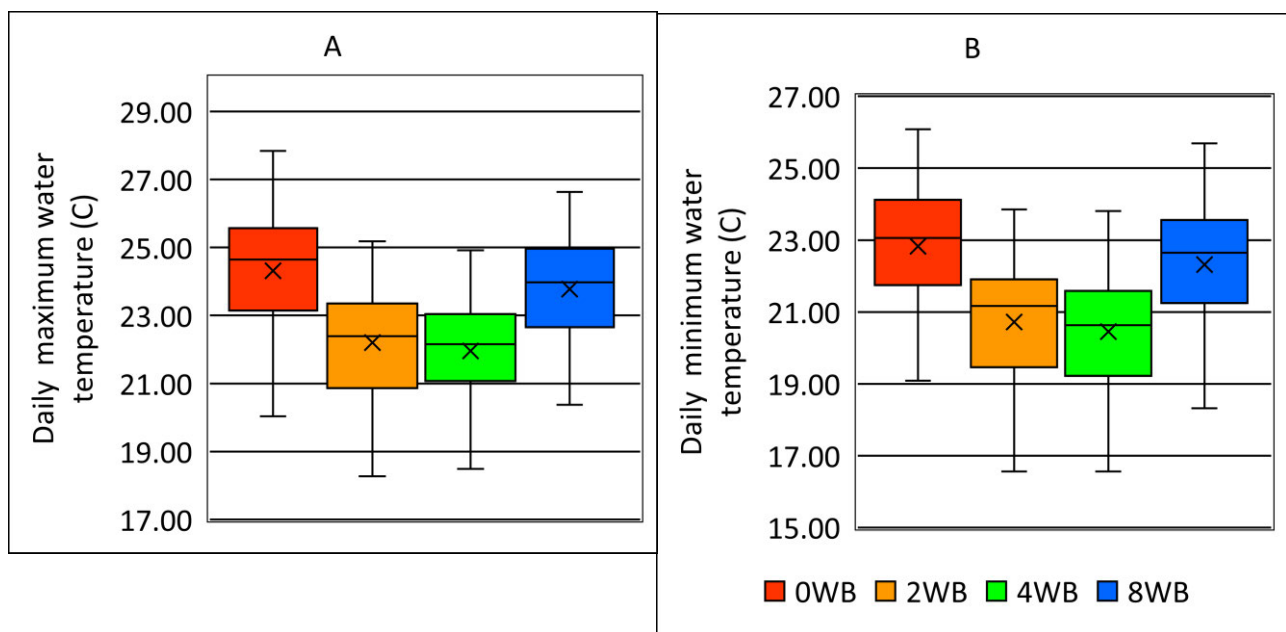
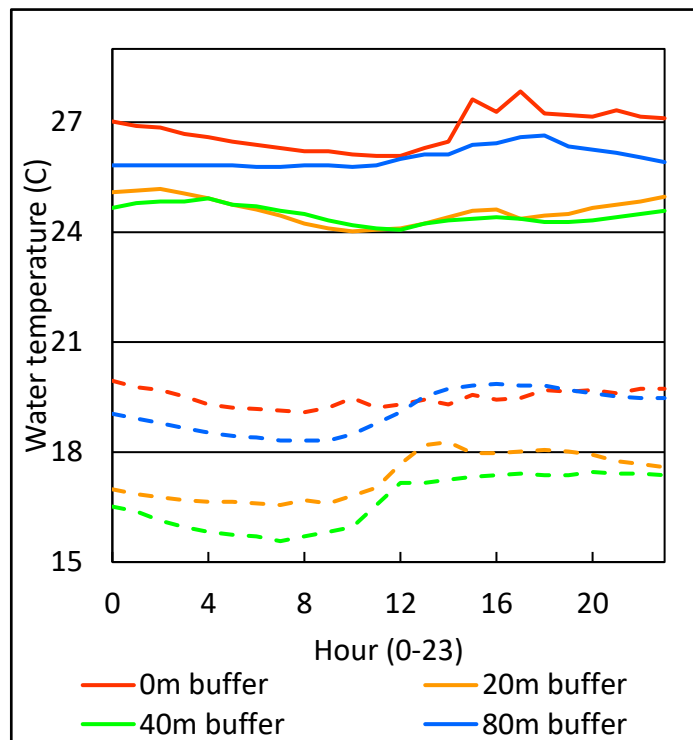


Figure 15: Mean maximum and minimum hourly water temperatures for each site. Maximum temperatures are indicated with a solid line, minimum temperatures are indicated with a dashed line.

3.2.2 Diurnal water temperature variation

Temperatures at the 0 m site and 80 m site reached maximum daily water temperature at a similar time with the 0 m site reaching a maximum of 27.8 °C at 5 PM while the 80 m site reached its maximum temperature of 26.6 – 26.64 °C between 5 to 6 PM respectively (Figure 15). In contrast the 20 m and 40 m sites reach their maximum daily water temperature at 2 AM (24.8 °C) and 4 AM (24.9 °C) respectively. Minimum hourly water temperatures do not share this contrast with each site of the vegetated zones sharing a similar trend of afternoon warming and a peak in the mid to late evening (Figure 15). The 0 m site varied to a smaller degree reaching its maximum of 19.95 °C at 0 AM (midnight) and only decreasing to its minimum daily temperature of 19.06 °C at 8 AM. In contrast the vegetated zones varied to a larger degree with the 20 m site varying 1.9 °C, the 40 m site varying 1.89 °C and the 80 m site varying 1.54 °C (Figure 15).

Figure 16: Daily maximum (A) and minimum (B) temperatures for each site. X indicate the mean, the middle line indicates median, the whiskers extend to the maximum and minimum.



3.3 GIS

3.3.1 Riparian vegetation inventory

The amount and characteristics of the riparian inventory along sections of South Creek can be summarised through buffer width and vegetation height. The width of the vegetated riparian zone was identified with areas of mean vegetation height ≥ 5 m. This found the Mamre location has the widest riparian width with a mean of 36 m followed by the Rossmore location with a mean width of 35 m and the largely unvegetated Twin Creeks location with an average width of 2 m (Figure 17).

Further analysis of the riparian inventory showed the Rossmore location has the highest mean riparian height within 15 m of the river channel at 8.2 m. This creates a total of 0.144 km² of vegetation cover ≥ 5 m high (Table 4, Figure 18A). This was followed closely by the Mamre location with an average height of 7.7 m covering 0.137 km². The Twin Creeks location was the lowest with a mean vegetation height of 3.5 m and vegetation ≥ 5 m covering an area of only 0.053 km² (Table 4, Figure 18A).

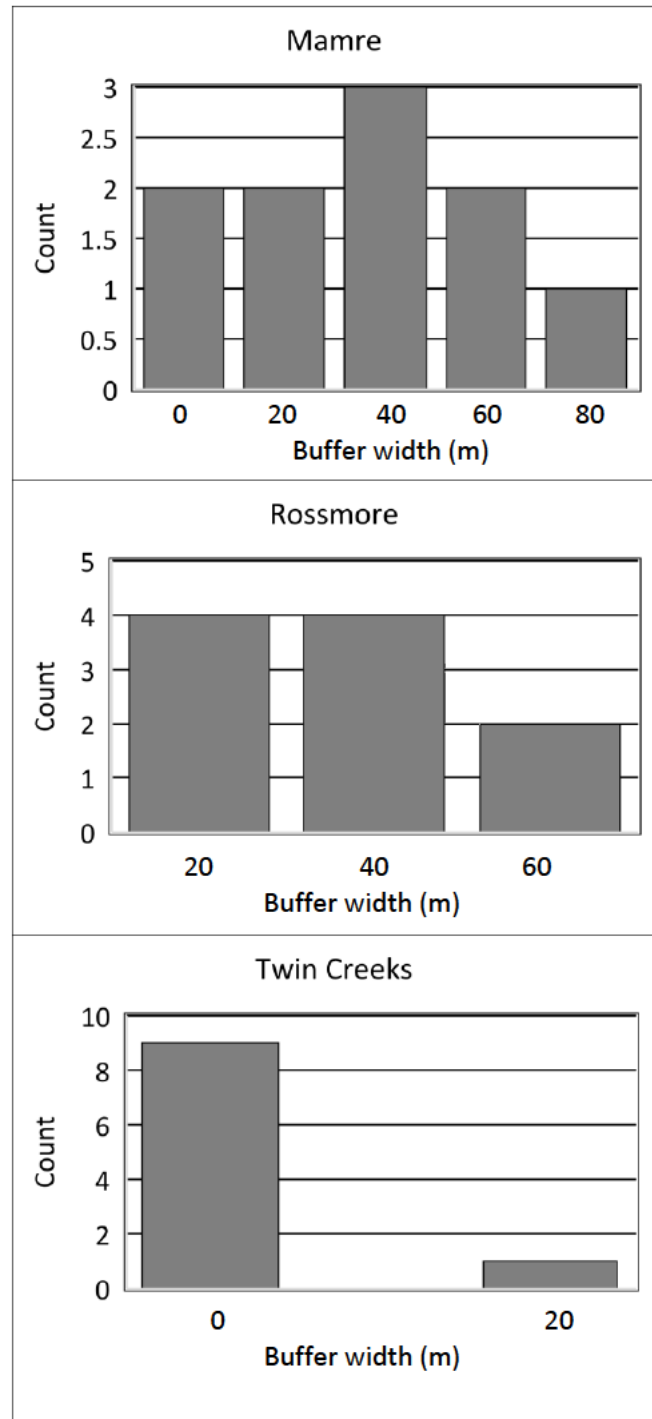


Figure 17: Riparian width for each location, areas with a vegetation height lower than 5 m were defined as non-riparian.

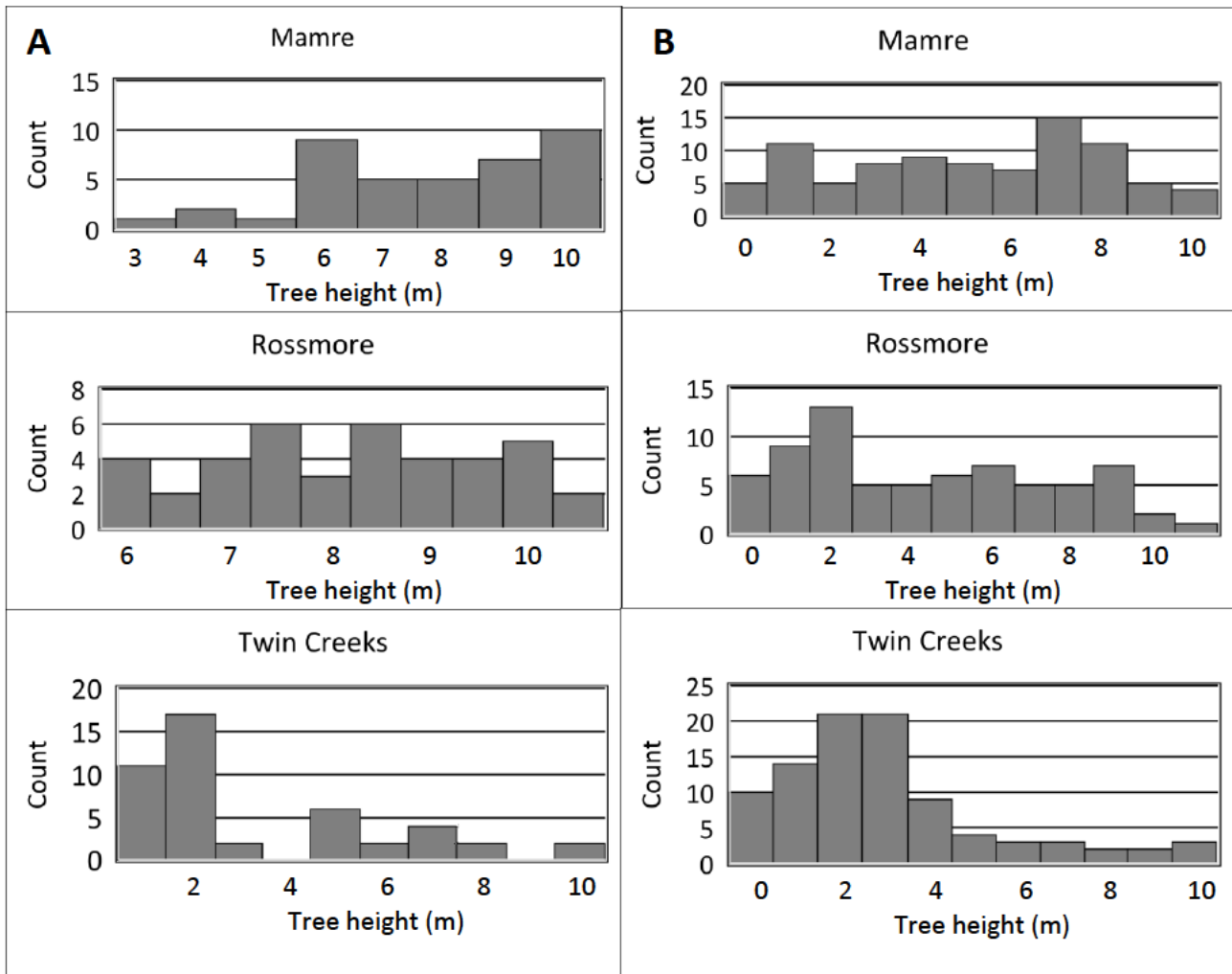


Figure 18: Vegetation height for each location within 15 m of the channel (A) and 80 m (B), height was limited to 10 m with larger values being rounded down.

Table 4: Vegetation height statistics for areas within 15 m of the stream and 80 m of the stream for each study location.

LOCATION		MAMRE	TWIN CREEKS	ROSSMORE
15 M	Mean (m)	7.729	3.518	8.232
	Interquartile Range (m)	6.2 - 9.7	1.5 - 5.2	7.2 - 9.4
	Sum ≥ 5 m (km ²)	0.137	0.053	0.144
80 M	Mean (m)	5.005	2.774	4.285
	Interquartile Range (m)	2.7 - 7.4	1.3 - 3.5	1.5 - 6.9
	Sum ≥ 5 m (km ²)	0.435	0.115	0.29

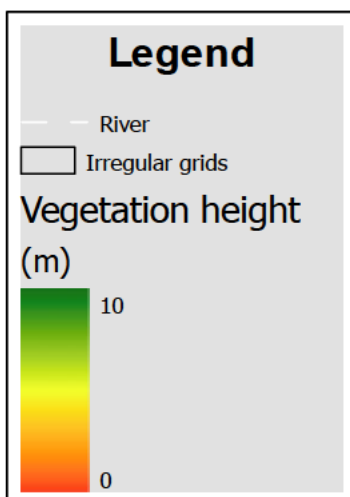
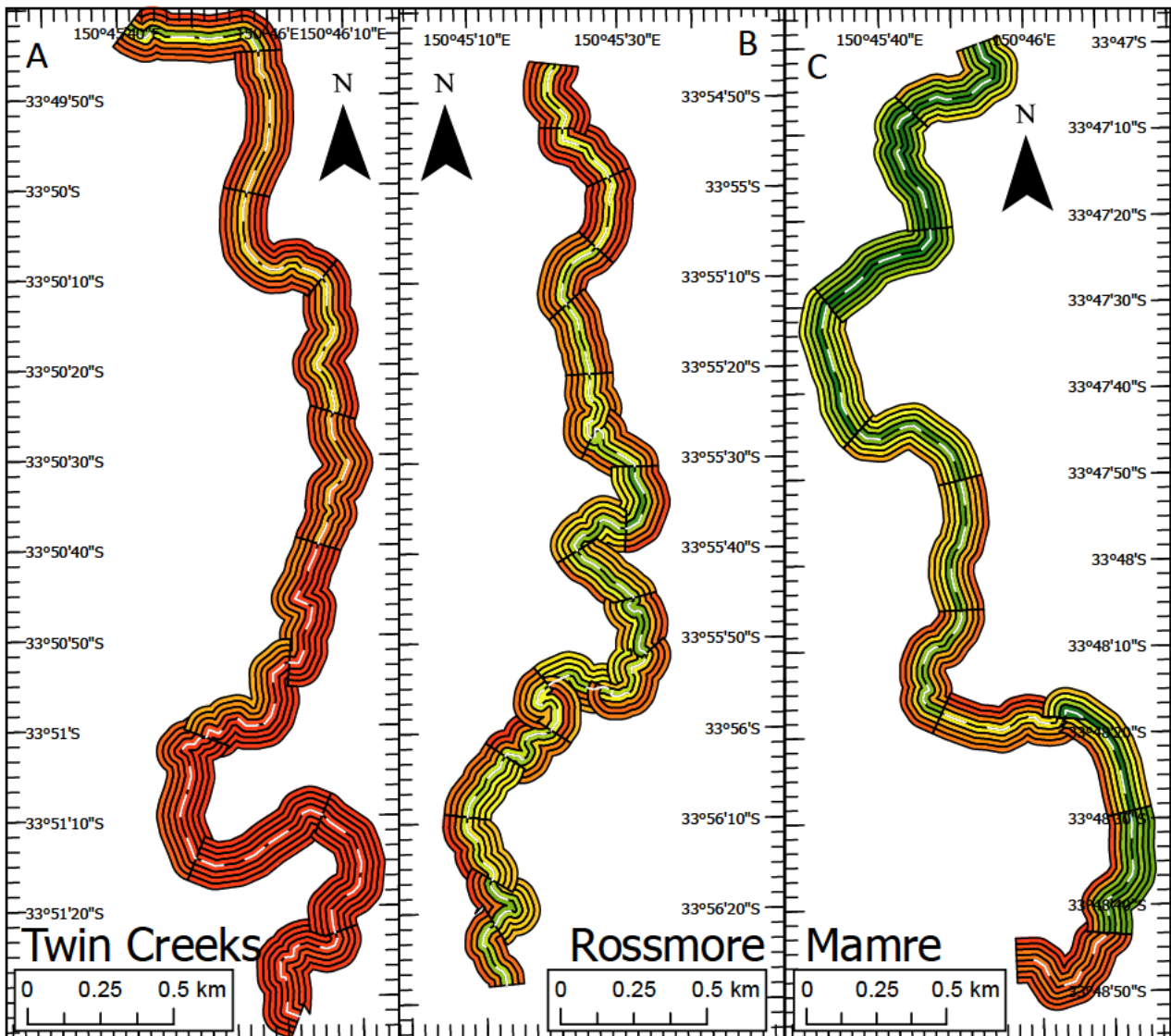


Figure 19: Riparian inventory for the 3 study locations based on mean vegetation height within each irregular grid section (~500x20 m), sections ≥ 5 m in height are classified as vegetated riparian zones.

When considering the riparian inventory within 80 m of the river channel, the Mamre location had both the highest mean vegetation height at 5 m and the largest area over 5 m at 0.5 km² (Table 4, Figure 18B). This was followed by the Rossmore location with a mean height of 4.3 m and covering an area of 0.29 km² with the Twin Creeks location lowest at 2.8 m and 0.1 km² respectively (Table 4, Figure 18B, Figure 19).

3.3.3 Riparian Cooling

Each of the temperature maps had higher mean daily maximum temperatures compared to the Badgerys Creek station mean daily maximum temperature for December 2022 of 28.5 °C (Bureau of Meteorology, 2023b). The Rossmore location had a higher mean daily maximum temperature of 29.2 °C while the Mamre location was higher at 29.7 °C across the 5 km modelled reach (Figure 20A, Figure 20B).

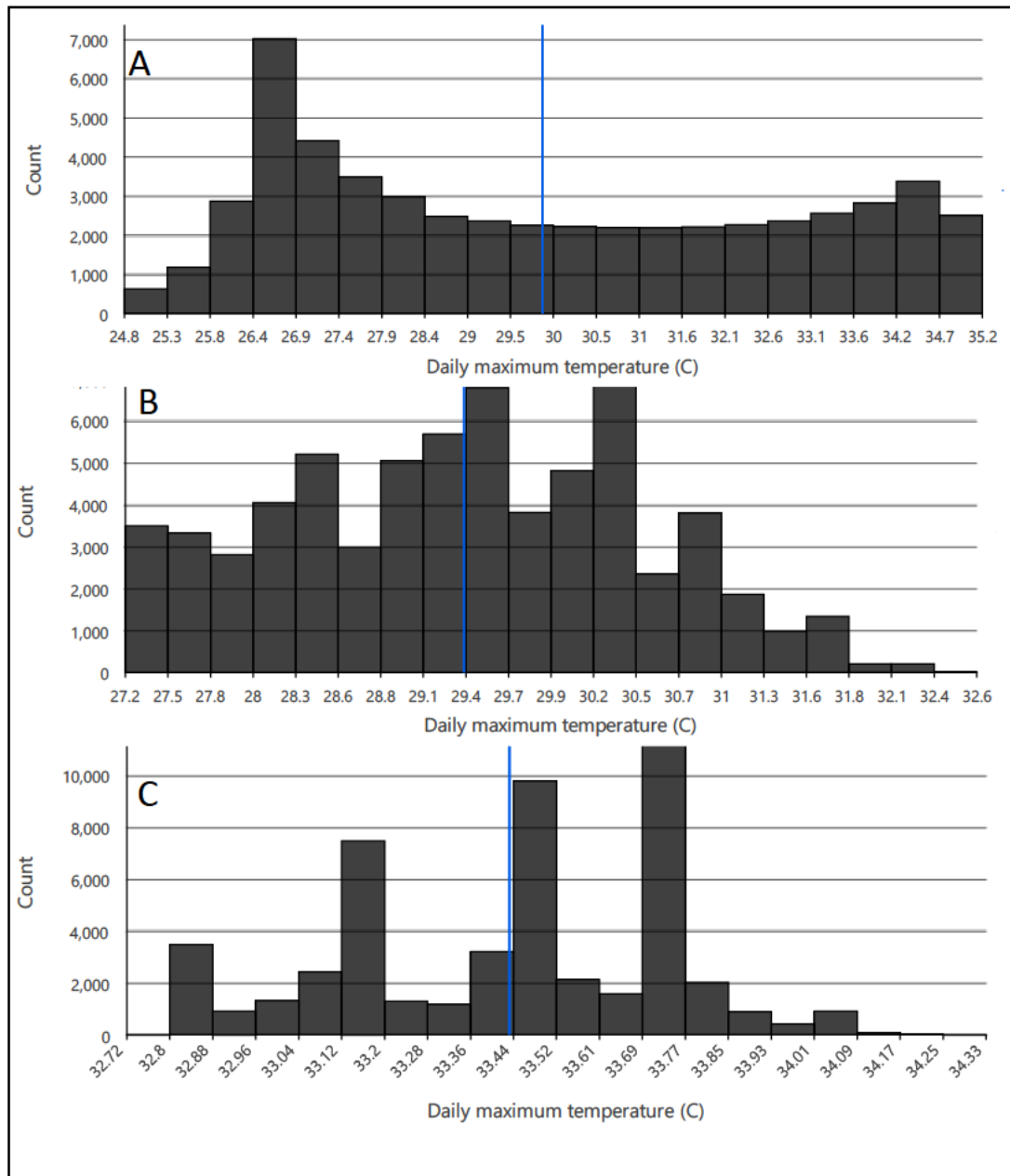


Figure 20: Modelled daily maximum air temperatures for Rossmore (A), Mamre existing (B) and Mamre unvegetated (C) conditions. Each count represents a raster pixel (5 m²), mean temperature is indicated in blue.

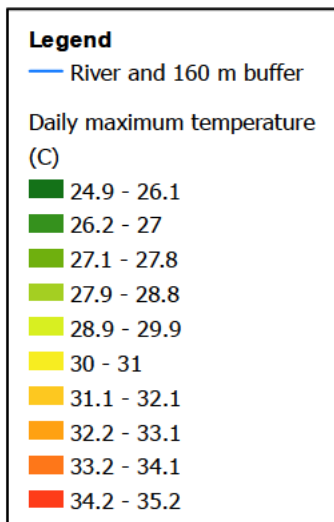
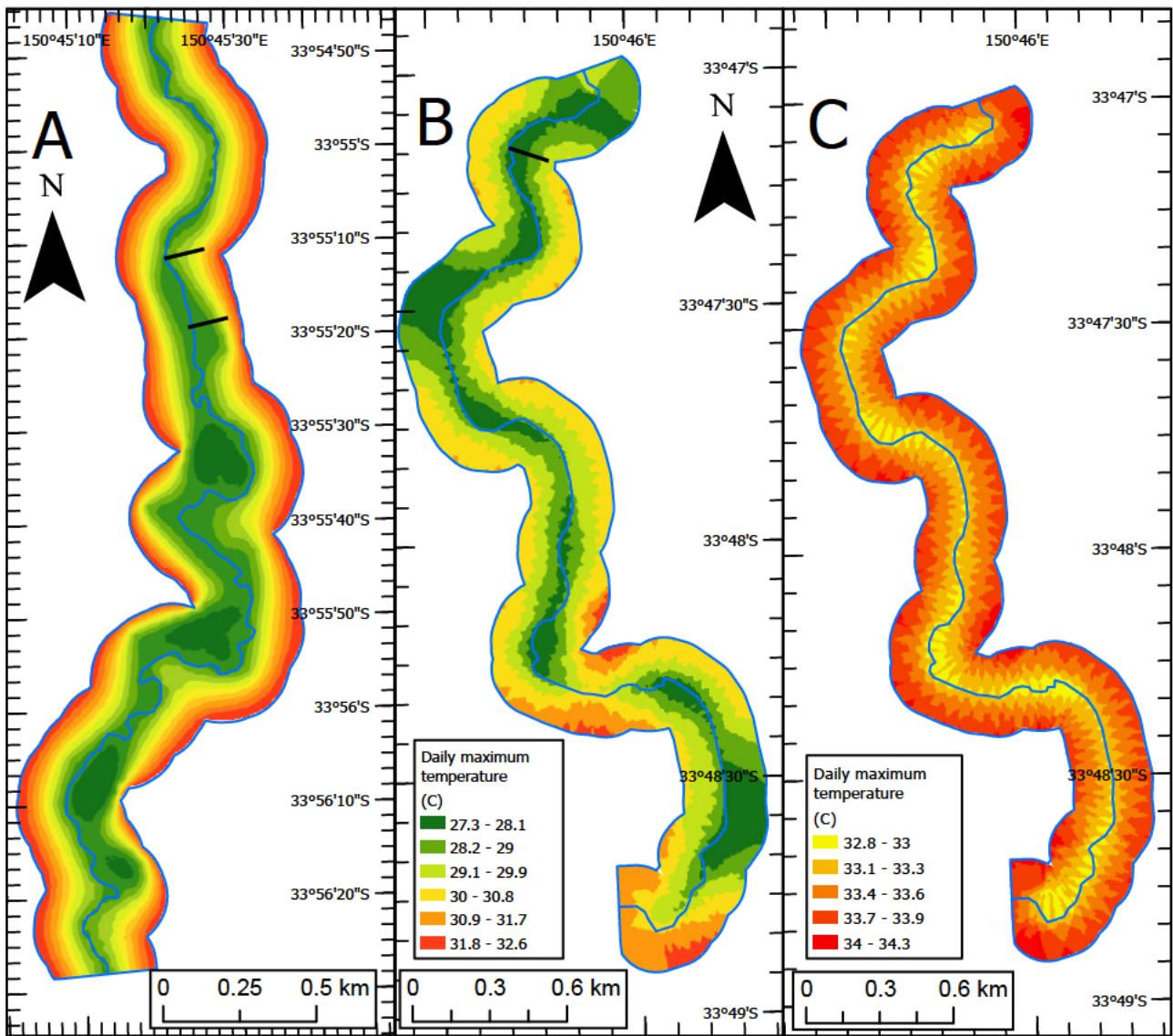


Figure 21: Modelled daily maximum air temperature maps for Rossmore (A), Mamre existing conditions (B) and Mamre with simulated no riparian buffer (C). In-field survey sites are highlighted in black.

The modelled unvegetated Mamre location was significantly ($P = 0.00$) hotter with mean daily maximum temperatures 4 °C higher, resulting in 1.5 km² of higher temperatures compared to the current vegetated conditions (Figure 20C, Figure 18).

The temperature maps (Figure 21) highlight cooler sections of riparian vegetation surrounding the vegetated sections visible, highlighted in the riparian inventory map (Figure 19). The coolest temperatures were located on the inside of the river bend or in the widest sections of the riparian

zone (Figure 21A, B). The modelled unvegetated Mamre location (Figure 21C) a spiking pattern in relation to the placement of the temperature points where temperatures of $\sim 31^{\circ}\text{C}$ would extend to 100 – 200 m from the river channel.

Each of the models compared poorly to their correlating in-field temperature gradients with the 20 m and 40 m buffer width zones modelled temperatures beyond the riparian zone being 4-6 $^{\circ}\text{C}$ cooler (Figure 22A, B). Temperatures across the Mamre reach more moderate across all distance from the river with temperatures only increasing 3 $^{\circ}\text{C}$ across the 150 m transect (Figure 22C). Temperatures along this transect were $\sim 2^{\circ}\text{C}$ warmer within the riparian zone and 2-4 $^{\circ}\text{C}$ cooler beyond the tree line.

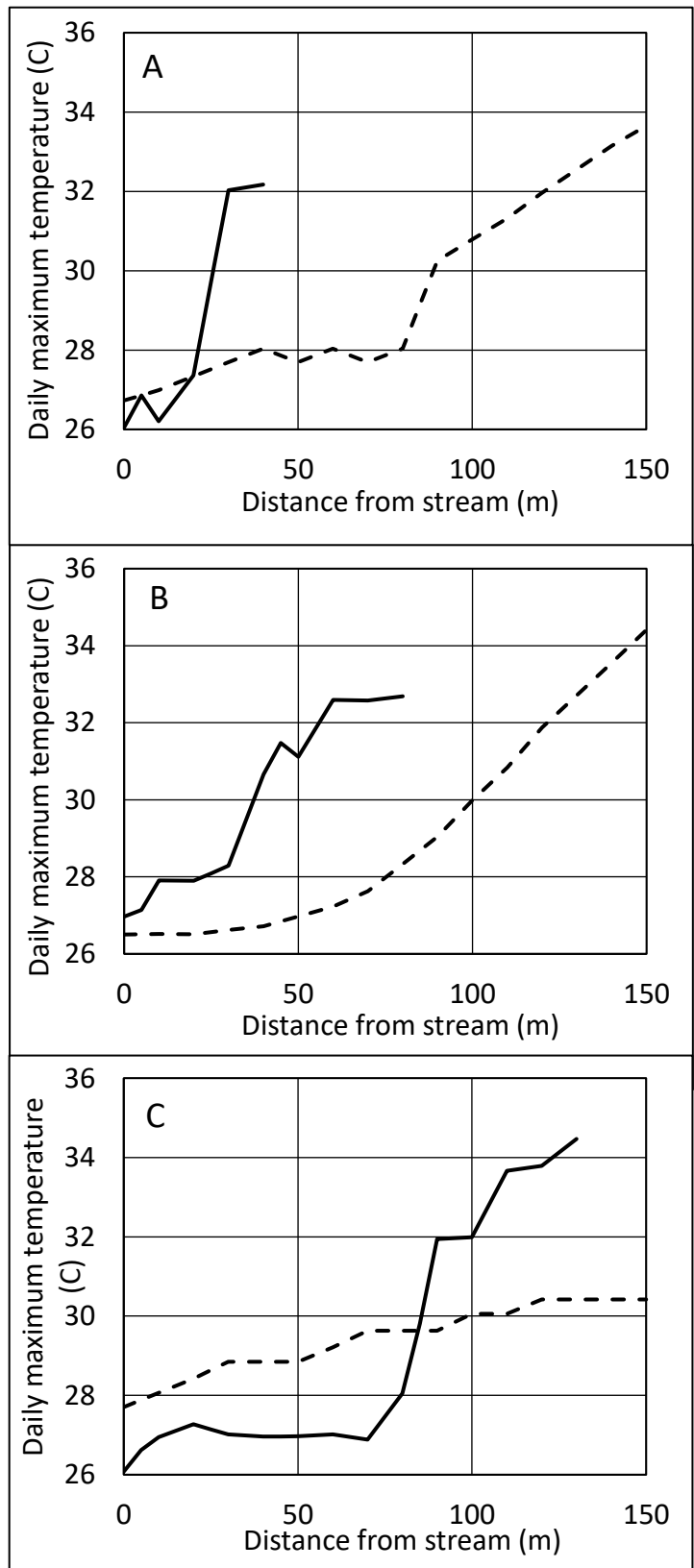


Figure 22: Modelled (dashed lines) and in-field (solid) daily maximum air temperatures gradients for sites with a 20 m buffer (A), 40 m buffer (B) and 80 m buffer (C).

4 Discussion

4.1 Riparian Microclimate

4.1.1 Bankside Air Temperatures

Each site featured the lowest temperatures adjacent to the river channel indicating the presence of a river channel effect that reduces daily maximum air temperatures. The extent of this is clearest when comparing temperature on the bankside with surrounding temperatures (Figure 11, Figure 12), where clear temperature gradients occur at bankside locations in the 0 m, 40 m, and 80 m sites.

The unvegetated 0 m site which has no riparian vegetation, only experienced a river channel effect that produced the largest reduction in daily maximum temperatures at nearly 5 °C within 5 m of the river channel. These findings are similar to others, including Rykken et al. (2007a) who found similar levels of cooling due to the river channel effect. It is possible that this warming also occurred within the first 5 m; however, their study included temperature sensors at only 0 m, 10 m, 30 m, and 70 m from the channel. Murakawa et al. (1991) also observed a strong river channel effect in the highly urbanised environment of Hiroshima, Japan where temperatures above the unvegetated Ota River were 5 °C cooler.

In this study along South Creek, vegetated sites (20 m, 40 m, 80 m) had lower bankside temperatures, due to both the cooling forces of the river channel and a riparian vegetation effect. Comparing temperatures across the riparian zone to the ~35 °C temperature plateau at the 0 m site indicates a ~6-7 °C decrease in daily maximum temperatures (Table 1) produced by the riparian vegetation effect (Figure 10, Figure 11). The immediate bankside temperatures of the vegetated sites indicate that the river channel effect only cools the vegetated sites a further ~1 °C. This indicates either a weaker river channel effect at vegetated sites or that the river channel and riparian vegetation effect do not compound effectively and can only reduce temperatures to a maximum of 8-9 °C instead of the expected 11-12 °C, based on the 5 °C river channel effect in the unvegetated zone and 6-7 °C riparian vegetation effect.

The decrease in river channel effect due to the presence of riparian vegetation is mirrored in Rykken et al. (2007a) who also saw more muted temperature gradients at bankside locations at their 30 m buffer and fully forested sites. In vegetated, lower order streams the river channel effect tends to have limited impact on temperatures (Brooks and Snowman, 2009). The Brooks and Snowman (2009) study on first to third order streams in New England, USA found no evidence of a temperature gradients within 30 m of the river channel. Differences in the quantitative findings of these studies

are likely due to differing study periods, forests, and stream types as well as differing regional climates to those occurring at South Creek (Brooks and Snowman, 2009; Yu et al., 2020).

In this study the river channel effect extended 10 m at the wider 40 m and 80 m sites compared to only 5 m at the unvegetated site. The spatial extent of the river channel effect is influenced by the presence of a riparian vegetation buffer, but this effect did not scale with increasing buffer width. This was not the case for the Rykken et al. (2007a) microclimate survey, with the river channel effect extending further at the fully forested site compared to the 30 m buffer. By contrast, in the Murakawa et al. (1991) study of the Ota River, cooling was present hundreds of meters from the river channel with the urban landform possibly promoting airflow and channelling of cool air, while larger waterbodies have also been found to generate stronger cooling (Du and Song, 2016).

The lack of a clear river channel effect at the 20 m site is likely due to a combined river channel, riparian and edge effects due to the smaller site size. This is seen in the riparian gradients over the common first 20 m distance (Figure 11, Figure 12A) with each of the vegetated sites sharing similar net temperature increases of ~ 1 °C in daily maximum temperatures within the first 20 m, except the 20 m site that experiences warming at the 20 m mark. For the 20 m site this warming is likely due to the edge effect rather than a diminishing river channel effect. This counterbalance in cooling / warming effects was found by Olson et al. (2007) in riparian microclimate studies in the American Pacific Northwest.

4.1.2 Riparian Air Temperatures

Air temperatures across the riparian zone were all significantly cooler than the unvegetated site, with maximum daily temperatures across the riparian zones being 6-5.5 °C cooler than mean temperatures for the unvegetated site. Along wider riparian zones, air temperatures plateaued further away from the influence of the river channel and edge effects (Figure 11). This produced large decreases in daily maximum temperature of between 6-7 °C at the 40 m and 80 m sites compared to the unvegetated site at similar distances from the river channel. These temperature plateaus persisted for 10 m from the riparian edge after which temperatures increased due to the edge effect.

Air temperatures across each of the riparian zones were also subject to significantly less temperature variation with daily maximum temperatures having lower standard deviation and

tighter inter quartile ranges (Table 1). This contrasts with the unvegetated site which was subject to extreme highs during hot days and similar temperatures to the vegetated sites during more moderate temperature days (Figure 9A). Figure 13B also displays this with minimum hourly temperature indicating 'cold days' where temperatures between 8 AM and 8 PM are ~ 1 °C warmer than at the unvegetated site, and ~ 5 °C warmer temperature for maximum hourly temperature or 'hot days'. The existence of a cooler riparian microclimate has also been found in other studies surveying different forest communities. Studies find similar results with riparian areas being 5-6 °C (Rykken et al., 2007a) or 6-9 °C (Anderson et al., 2007) cooler than cleared or unvegetated locations. Additionally, Tsai et al. (2017) found that the difference between riparian and non-riparian locations to be greater during summer and "extreme hot weather", which for their study site in Sheffield, UK was 27.4 °C.

The impact of buffer width on the magnitude of cooling due to the riparian vegetation effect can be found by comparing temperatures across the riparian zones for each of the vegetated sites. This would indicate no relationship between riparian effect strength and buffer width size with the 20 m and 80 m sites having statistically similar mean riparian daily maximum temperatures (Figure 10) despite the large size difference. However, the lower temperatures found in the smallest riparian zone (20 m width) may be due to over representation of the river channel effect. With the 40 m and 80 m sites covering larger distances, a smaller proportion of the sensor arrays are impacted by the ~ 10 m of cooler temperatures from the river channel effect. On the other hand, a larger proportion of the 20 m site is subject to warmer temperatures due to the edge effect with half of the 20 m riparian zone within 10 m of the warmer adjacent field.

The overlapping effects along the 20 m riparian zone produced no clear temperature gradients or plateaus for daily maximum temperatures and therefore it is challenging to isolate the contribution of just the riparian vegetation effect (Figure 11). While low temperatures present here may be due to local factors, the 20 m and 40 m sites were within 1 km of each other and featured very similar vegetation communities and channel characteristics. A possible explanation for these low temperatures is better airflow along the riparian zone, resulting in a less powerful but more extensive river channel effect that covers the whole riparian zone. A study of urban greenspace in Leipzig, Germany found similar interactions with smaller greenspaces better mixing with surrounding air compared to larger greenspaces. In the urban context, this resulted in warmer greenspace temperatures and cooler surroundings as the cool air of the greenspace was better mixed with the surrounding hot urban air (Jaganmohan et al., 2016).

The 40 m and 80 m sites feature very similar temperature gradients across their riparian zones despite the difference in scale. However, the riparian vegetation effect at the 80 m site created significantly lower mean daily maximum temperatures (Table 1). The increase in width from the 40 m to 80 m riparian zones resulted in a more robust microclimate with daily maximum temperatures being significantly cooler at the wider site with a plateau temperature being ~ 1 °C cooler. The 80 m site was also able to maintain internal temperatures more effectively overnight, resulting in significantly higher daily minimum temperatures (Figure 13B). This can be attributed to either a more powerful riparian vegetation effect at the larger site or changes in airflow due to the larger size producing a more intact riparian microclimate.

The Jaganmohan et al. (2016) study on greenspaces of varying sizes also found that larger zones exhibited more consistent and cooler temperatures due to less cool air being transported away from the microclimate. It is important to note that the Jaganmohan et al. (2016) study considered urban forests and parks of much larger size range than what was analysed along South Creek, with a median of 2.2 ha and a maximum size of 35 ha. However, the Jaganmohan et al. (2016) findings of scaled cooling intensity with size are consistent with other studies where larger sites produce more intense and extending cooling (Chang et al., 2007; Yu et al., 2021). However significant cooling effects were also found in smaller greenspace sizes of 0.1 ha to 1 ha (Jaganmohan et al., 2016; Fan et al., 2019). Additionally Olden et al. (2019) found larger buffer widths were more resilient to the logging of surrounding forests, recommending buffer widths larger than 30 m are needed to protect the riparian microclimate (Olden et al., 2019). Kong et al. (2014) found the same with larger greenspaces forming more stable internal microclimates.

The impact of the edge effect was also visible across each of the vegetated sites, highlighted in Figure 11B. As discussed, temperature gradients across the 20 m riparian zone can be attributed to a combination of effects, however the temperatures increase within 10 m of the riparian zone edge, consistent with the other sites regardless of buffer width (Figure 11, Figure 12A). Temperatures within 10 m of the riparian edge at the 40 m zone features the largest degree of warming compared to 20 m and 80 m sites. This is attributed to the 20 m site featuring better airflow and an extended river channel effect, and the 80 m site featuring a more powerful riparian vegetation effect, in both cases resulting in a poorly expressed edge effect.

4.1.3 Field Air Temperatures

Air temperatures outside the riparian zone were characterised by the extent of the riparian vegetation effect against prevailing background temperatures, with the 0 m unvegetated site experiencing only the river channel effect as discussed earlier. For the vegetated sites, air temperatures increased to a plateau at ~ 32 °C for the 20 m site and 32.5 °C at the 40 m site. Temperatures briefly plateau at 90 – 100 m at the 80 m site also at ~ 32 °C (Figure 11). However, at the 80m site the temperature continues to increase towards similar temperatures experienced at the unvegetated site. Due to the limited survey extent of the 20 m site extending to a total of only 40 m from the river channel, its temperature plateau extending only 10 m it's possible that temperatures would further increase beyond this point. However, with both the 20 m and 40 m sites reaching similar plateau temperatures could indicate the impact of regional background temperatures that prevent temperatures from increasing further to 35 °C seen at the 0 m and 80 m sites. This suggests that the temperature plateau seen is not a product of the riparian effect, but rather another variable reducing temperatures. This could be due to differing vegetation communities of the field sections with the 80 m site featuring shorter pasture grasses in contrast to the taller, denser, and unmanaged grasses at the 20m and 40 m sites. The difference in grass; species, height, and evapotranspiration and this impact in soil and air temperatures remains largely unexplored.

The strength and range of the riparian vegetation effect can be interpreted from the linear temperature gradients based on the common 20 m distance beyond the riparian zone (Figure 11, Figure 12B). The 20 m, 40 m and 80 m sites all feature high rates of air temperature increase within the first 20 m of the field, suggesting that the extent of the riparian vegetation effect is not influenced by the size of the riparian buffer. This is opposite of what was observed for internal riparian temperatures discussed earlier and in other studies (Chang et al., 2007; Jaganmohan et al., 2016; Olden et al., 2019). When solely comparing the shallower temperature gradients for the 40 m site to the smaller 20 m site there is evidence of a 'buffer width size' to 'riparian effect extent' relationship. As both these zones share similar vegetation communities and background temperatures, comparisons between these two sites better represents the impact of buffer width. The differing field vegetation at the 80 m site could potentially explain why this trend is not evident there. Ignoring the temperature itself and only focussing on the temperature gradient can account for this difference in vegetation and background or plateau temperature at the 80 m site. Due to the lack of a clear temperature plateau along the 80 m transect, it is possible that a plateau of >35

°C was never reached and lies beyond the survey extent. This supports the argument that larger buffer widths have a riparian vegetation effect that extends further, as temperatures at the 80 m site continue to increase up to the survey extent of 40 m (Figure 11).

4.1.4 Minimum Air Temperatures

Although heat mitigation is this studied focus, daily minimum temperatures highlight how both the river channel and riparian vegetation effect warm the surrounding areas overnight. This produces a blanket like influence on temperatures. Possible explanations for the warming effects in riparian zones include better overnight heat retention in the river and riparian microclimate (Theeuwes et al., 2013) due to higher humidity levels and a higher heat capacity (Oke, 1973; Murakawa et al., 1991; Theeuwes et al., 2013). This limits the rate of daytime warming and the decline in temperature overnight. This trend is visible in the flatter diurnal variation gradients for the vegetated sites (Figure 13A).

In bankside environments the river channel effect produced warmer overnight temperatures with higher bankside daily minimum temperatures at the 0 m, 20 m, and 40 m site. The unvegetated site showed the river channel effect increased temperatures by 1 °C within 5 m of the channel bank. Again, the vegetated sites were subject to both the river channel and riparian vegetation effect. However, the 20 m now site shows clear separate gradients for the river channel and riparian vegetation effects (Figure 11). A similar effect was found by Rykken et al. (2007a) who found 6 AM bankside temperatures to be ~ 1 °C warmer at unvegetated locations and ~2 °C at vegetated locations. Additionally, temperatures in their 30 m riparian zone remained 2 °C cooler along the extent of the buffer (Rykken et al., 2007a). Tsai et al. (2017) also observed a 2 °C warming effect in urban riparian zones, with rural sites being marginally (0.1-0.2 °C) warmer. Differences between riparian and non-riparian minimum temperatures were found to be more pronounced during very cold winters (Tsai et al., 2017), conditions that are not experienced in South Creek or Greater Sydney.

This study found that the river channel effect seems to be less effective along larger buffer widths, increasing temperatures by 0.9 °C at the 20 m site within 5 m and 0.4 m within 10 m at the 40 m site. At the widest 80 m site, minimum temperatures increased at 10 m indicating that the river channel effect was substantially less effective compared to riparian vegetation effect.

Another explanation for this decrease in river channel effect could be the balance between river channel and riparian vegetation effects, with wider zones forming more robust and intact riparian microclimate, better heat retention resulting in warmer minimum temperatures and a less pronounced river channel effect. The statistically similar temperatures across the 20 and 40 m riparian zones suggest that wider riparian vegetation buffers are needed to form a more robust riparian microclimate that can mitigate daily temperature extremes by retaining more heat over night. This is further supported by the 80 m field being significantly warmer than the other sites, with the 20 m site being slightly warmer and the 40 m site being slightly colder, indicating no relationship between buffer width and minimum temperatures or effectiveness of the riparian vegetation effect for these narrower zones. Jaganmohan et al. (2016) found that the warming effects of urban greenspaces was significantly influenced by size however many greenspaces failed to produce any overnight warming effect. This contrasts to other studies from Rykken et al. (2007a) and Tsai et al. (2017) that find similar warmer conditions at vegetated riparian zones.

4.2 Water Temperatures

Although a significant proportion of a rivers' thermal regime is dependent on solar input and by extension the characteristics of the riparian vegetation (Moore et al., 2005; Caissie, 2006), there are other variables that can influence water temperature such as discharge, channel volume and upstream water temperature that were beyond the scope of this study. As a result, we did not expect to see a clear correlation between buffer width and water temperatures. Therefore, the focus here is solely on the differences between the vegetated and unvegetated sites to determine the impact of a riparian buffer.

As expected, the presence of a riparian buffer also resulted in significantly lower daily maximum and minimum water temperatures in the vegetated sites (Table 3) due to the interception of incoming solar radiation by the channel side vegetation. The increased temperatures can be attributed to afternoon solar input, with maximum hourly temperatures spiking at 3 – 5 PM at the unvegetated sites, whereas the vegetated sites featured a much flatter temperature gradient across the day (Figure 17). Additionally, the more moderate decreases in daily maximum temperature at the 80 m site compared to 20 and 40 m sites may be due to upstream conditions where upstream water carries the thermal conditions of that reach into the following downstream reaches (Moore et al., 2005). The 80 m site features some unvegetated sections upstream of our water temperature

sensors identified by our riparian inventory map (Figure 19C), additionally the 80 m site was downstream of the highly unvegetated Rossmore reach (Figure 19A). In contrast the 20 and 40 m sites were downstream of more consistently intact riparian zone (Figure 19B).

Several studies have examined the impact riparian zones have on water temperature by comparing vegetated to cleared reaches before and after clear cutting (Moore et al., 2005). The Moore et al. (2005) review looking at water temperatures post-forest harvesting and found that temperatures consistently increased, ranging from ~ 10 °C at clear cut locations with more moderate $\sim 2-5$ °C increases at locations containing buffers (Moore et al., 2005).

4.3 Riparian Mapping

4.3.1 Riparian Inventory

The LiDAR data used in this study was able to effectively characterize the riparian conditions across each of the selected study reaches with vegetation height being presented in “Rivergraph polygons”. This success is consistent with other studies that use LiDAR DEM’s to characterize and map riparian vegetation (Wawryniak et al., 2017; Loicq et al., 2018). This concurs with the Dugdale (2019) study that finds LiDAR DEM surveying to be one of the most effective and accurate methods.

Each of the study site showed varying riparian conditions within 80 m of the river channel, with the Twin Creeks showing a typical agricultural setting featuring unvegetated grazing land adjacent to a river channel (Figure 17, Figure 18, Figure 19). The Rossmore and Mamre sites featured much higher levels of vegetation, the key difference being the consistency of the buffer zone vs width of the buffer, with the Rossmore site featuring a more complete riparian vegetation buffer while the Mamre site had larger riparian zone (Figure 17, Figure 19). These results highlight areas where the buffer width is under the government guidelines, which in this case recommend a width of at least 40 m (Department of Planning and Environment, 2022a). This difference is also highlighted in the mean vegetation height analysis (Figure 18) with the Rossmore site featuring a higher mean height within 15 m of the river channel compared to the Mamre site, resulting in an additional 7,000 m² of wooded riparian vegetation. Expanding this to 80 m from the river channel, the Mamre site has the higher mean vegetation height and an additional 0.2 km² of riparian vegetation, indicating wider buffer zones at the Mamre site while the Rossmore site featuring more grassland (Table 4). A limitation of mean vegetation height analysis is the lack of distinction between continuous riparian

zones and other vegetation elements within the survey area. However, limiting this survey to 15m or 80 m from the river channel would exclude much of the non-riparian vegetation.

4.3.2 Temperature overlay

With the use of the remotely sensed riparian buffer width, air temperatures were approximated using the in-field collected data. The temperature overlay maps expand the findings of the 1-dimensional surveys into 2 dimensions, covering larger areas of the surrounding environment (Figure 21). Due to a similar magnitude of cooling experienced across the vegetated sites regardless of width these maps were mainly focused on portraying the difference to total area cooled and how temperatures shifted along the riparian corridor. With this goal in mind the temperature maps were effective at portraying this difference, especially when examining the vegetated and unvegetated sections of Mamre (33°38'S - 33°48'30"S) (Figure 21B). However, the modelled temperatures produced much lower temperatures when compared to the in-field records, especially for locations beyond the riparian zone (Figure 20, Figure 22).

The vegetated and unvegetated models at Mamre also communicate the impact of riparian cooling (Figure 20B, C), with existing conditions having significantly cooler mean daily maximum temperatures ($P=0.00$) resulting in 1.5 km² of cooler temperatures. Based on our in-field collected data (Figure 5) differences between the vegetated and unvegetated Mamre reaches should indicate a 6 °C difference in the riparian zone and a ~3 °C difference beyond the riparian zone (Table 1). Temperatures were instead only 3.5-4.5 °C across the entire survey area. This overestimation of the extent of riparian cooling in the models was due to the more linear temperature gradients between the bank, riparian edge, and survey extent. The magnitude of cooling was moderate at either end of the temperature transects with warmer than expected bankside temperatures and cooler temperatures at the survey extent (Figure 22B, C). The 20 m site was the only location that featured modelled a significant temperature shift with temperatures increasing 2 °C 80 m beyond the channel (Figure 22A). The lack of temperature gradients at the riverbank and riparian edge result in the over and underestimation of temperatures. Increasing the difference in temperatures for each of the temperature points could better portray the difference between riparian and field locations. Additionally, increasing the number of points along the bank, riparian edge and survey extent as well as including points at the established bounds of the river channel effect and riparian vegetation effect to force the temperature gradients found in the field collected data. Furthermore, the

inclusion of additional variables like humidity, elevation, vegetation “nativeness”, and surface composition for urban areas might better project temperatures and improve the applicability of this model.

Additional models for each location were created using ArcGIS Pro’s statistical wizard which tailors the interpolation variables to improve standard error and root-mean-square. However, although these maps had better accuracy in reference to the temperature points, they still struggled to portray the temperature gradients observed in the field. The chosen method was more effective at highlighting the temperature difference between vegetated sections and areas without riparian vegetation. Additionally, these maps highlight the spatial differences between each of the buffer widths with larger zones cooling larger areas.

4.4 Implications for urban planning, stream management and UHI mitigation

The findings of the temperature surveys are presented in Figure 23. These findings highlight the cooling impact of riparian vegetation in the riparian zone and adjacent fields and can be used alongside the temperature maps to better communicate the impact of riparian vegetation on air and water temperatures.

With the apparent limited reach of the river channel effect, most of the cooling experienced was due to the riparian vegetation effect. The lack of relationship between width and the magnitude of cooling from the riparian vegetation effect would suggest that riparian zones of 20 m more effectively cool the surrounding environment. The ability for even small zones to significantly reduce local temperatures increases the applicability of riparian greenspace as a tool to combat UHI as smaller zones are more common in these settings (Fan et al., 2019; Yu et al., 2021). Meanwhile, wider riparian zones do more effectively cool larger areas and their effects extend a lot further. Yu et al. (2021) found similar results when studying green and blue space in Nanning, China with smaller sites (~0.3 ha in size) being the most efficient at cooling due to the logarithmic cooling to size relationship, even though temperatures were lower at larger sites. This basis for cooling effectiveness is the reduction of internal microclimate temperatures. However how the riparian effect extends and cools the surrounding area is also an important consideration for UHI focused riparian zones. At South Creek, larger zones were more effective at reducing surrounding temperatures with the 80 m site showing signs of reducing air temperatures 40 m beyond the riparian zone. The 40 m site was found to have a marginal impact on surrounding temperature and

had the warmest riparian zone. Consequently, riparian zones should target a buffer width of either 20 m or 80 m where possible to maximize the cooling benefits of the riparian vegetation and river channel effects. As the greenspaces studied were surrounded by grasslands, it is anticipated that greater cooling would occur at more urbanized sites due to the higher background temperatures with temperature differences being more pronounced on hotter days (Figure 13). Tsai et al. (2017) compared riparian cooling across rural and urban areas found similar results with maximum daily temperatures consistently higher at urban locations. Furthermore, larger scale cooling from both the river channel and riparian vegetation effect is also anticipated to extend beyond the survey extents of our sensor transects with studies finding cooling to extend the river channel effect by 40 – 100 m (Park and Lee, 2019) with possible small-scale cooling from blue green space extending 500+ m (Jiang et al., 2020).

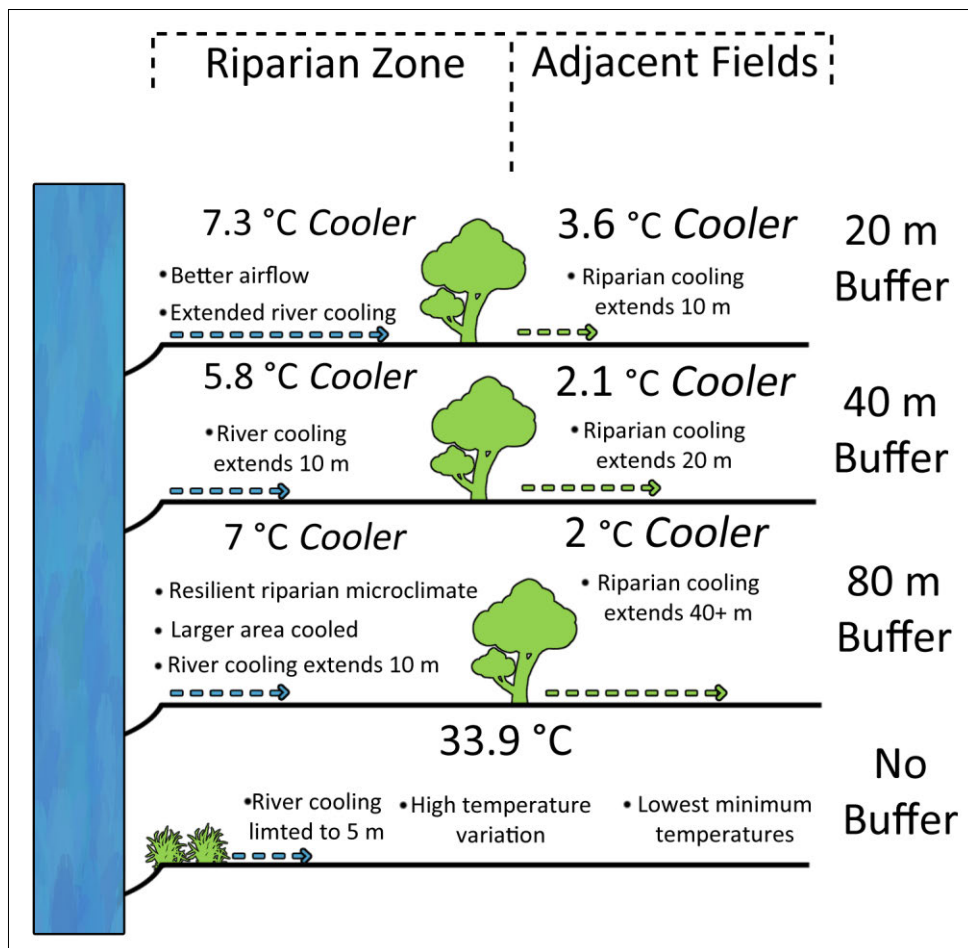


Figure 23: Comparison of daily maximum temperatures between buffer widths. Dashed lines indicate river channel effect (blue) and riparian vegetation effect (green) extent.

For implementation in the Western Sydney region, these results can help guide development to properly utilize existing green spaces and ensure new green spaces are effective at reducing temperatures and mitigating UHI. The Greater Sydney regional plan features several sustainability priorities, many of which are focused on protecting natural bushland and addressing the issues of UHI (Greater Sydney Commission, 2018b). Many of these priorities are culminated in the South Creek corridor plan which aims to create a continuous vegetated riparian corridor along the newly urbanized catchment. Importantly these plans highlight a variety of areas including city centers, industrial parks and suburbs built around the riparian corridor, however they do not include targets for the width of the riparian corridor and the type of vegetation present (Greater Sydney Commission, 2018b). The results of this study could be built into these green space plans; by first identifying the existing riparian conditions, highlighting areas where the existing buffer is under the NSW guidelines of 40+ m (Department of Planning and Environment, 2022a). Additionally, the microclimate surveys better quantify the cooling impact that riparian zones have, by breaking down these hybrid blue / green spaces into the river channel, riparian vegetation, and edge effects. The differences in microclimate effects for buffers of different width changes how the cooling is expressed with the 20 m zone seemingly behaving differently to the larger 40 m and 80 m buffers. Importantly this should guide the target buffer width for the proposed corridor when the goal of these spaces is to mitigate UHI. As established by other studies and reaffirmed by the findings in this study, even small sections (<0.3 ha or 20 m buffer widths) of greenspace can significantly reduce daily maximum temperatures, with larger sections experiencing a higher consistency of cooling that extends further into adjacent areas (Chang et al., 2007; Jaganmohan et al., 2016; Fan et al., 2019; Olden et al., 2019). Depending on the land use and the space available, the target buffer width for forested riparian corridors can be as small as 20 m, as these sites significantly decrease internal daily maximum temperatures as well as the immediate surrounding area. Although the impact of paths, and other breaks in the riparian canopy showed no effect on temperatures at the 40 m site, the impact of these potentially disruptions to the riparian microclimate need to be studied further (Tsai et al., 2012; Liang et al., 2021) with any structure potentially breaking the cohesion of smaller riparian zones, diminishing their cooling effect (Tsai et al., 2012; Jaganmohan et al., 2016; Liang et al., 2021). For this reason, larger zones would be better suited for providing a space for recreational activities or as commuting pathways which are not subject to extreme heat. Additionally, these larger zones would more effectively reduce the temperatures of surrounding unforested recreational areas and adjacent buildings.

5. Conclusions

This study reveals riparian microclimate temperatures in a high spatial resolution and effectively characterizes the forces that act to reduce air temperatures. The four sites analysed highlight different riparian conditions present along South Creek in western Sydney. Each location produced different temperature microclimates due to variation in the strength and extent of the river channel, riparian vegetation and edge effects present along the stream. This resulted in a significantly hotter unvegetated site compared to the sites featuring larger forested riparian buffers, confirming our first hypothesis regarding the impact of present or absent riparian vegetation. Variation between each of the vegetated riparian zones due to their difference in width partly confirmed our second hypothesis, however the relationship between buffer width and cooling experienced was not as linear as predicted. While the narrow 20 m riparian zone created the coolest temperatures, the increase in buffer width from 40 m to 80 m resulted in a more robust microclimate with lower temperature variation and resistance from outside air temperatures. Furthermore, the increase in buffer width from 20 m to 40 m and 80 m resulted in the riparian vegetation effect reducing temperatures of the adjacent cleared fields and extending further, confirming our third hypothesis. Other studies could look into changes in other microenvironment variables such as soil temperature and moisture, relative humidity, and solar exposure to better understand how buffer width impacts the riparian microclimate. The remotely sensed LiDAR data was able to quantify the existing riparian buffer conditions along sections of South Creek, with these techniques available to be applied on a catchment scale. Modelling the infield air temperature data highlighted the spatial coverage and extent of cooling due to the river and riparian vegetation, however further research is needed to improve the accuracy of these models.

References

1. Anderson, B. G., Rutherford, I. D., and Western, A. W. (2006) An analysis of the influence of riparian vegetation on the propagation of flood waves. *Environmental Modelling and Software: with Environment Data News*, 21(9): 1290–1296.
<https://doi.org/10.1016/j.envsoft.2005.04.027>
2. Anderson, P. D., Larson, D. J. and Chan, S. S. (2007) Riparian buffer and density management influences on microclimate of young headwater forests of western Oregon. *Forest Science*, 53(2): 254-269.
3. Balcombe, S. R., Sheldon, F., Capon, S. J., Bond, N. R., Hadwen, W. L., Marsh, N. and Bernays, S. J. (2011) Climate-change threats to native fish in degraded rivers and floodplains of the Murray-Darling Basin, Australia. *Marine and Freshwater Research*, 62(9): 1099–1114.
<https://doi.org/10.1071/MF11059>
4. Benson, D. H. and Howell, J. (1990) *Taken for granted: the bushland of Sydney and its suburbs*. Kenthurst, N.S.W: Kangaroo Press in association with the Royal Botanic Gardens Sydney.
5. Booth, D. B., Karr, J. R., Schauman, S., Konrad, C. P., Morley, S. A., Larson, M. G., and Burges, S. J. (2004) Reviving urban streams: land use, hydrology, biology, and human behavior. *Journal of the American Water Resources Association*, 40(5): 1351–1364. <https://doi.org/10.1111/j.1752-1688.2004.tb01591.x>
6. Boyd, M. and Kasper, B. (2003) *Analytical methods for dynamic open channel heat and mass transfer: Methodology for heat source model version 7.0*. Portland, Oregon Department of Environmental Quality.
7. Boyd, M. and Kasper, B. (2003) Analytical Methods for Dynamic Open Channel Heat and Mass Transfer: Methodology for the Heat Source Model Version 7.0. <http://www.deq.state.or.us/wq/TMDLs/tools.htm>.
8. Brierley, G. J., Cohen, T., Fryirs, K., and Brooks, A. (1999) Post-European changes to the fluvial geomorphology of Bega catchment, Australia: implications for river ecology. *Freshwater Biology*: 41(4), 839–848. <https://doi.org/10.1046/j.1365-2427.1999.00397.x>.
9. Brooks, R. T. and Kyker-Snowman, T. D. (2009) Forest-floor temperatures and soil moisture across riparian zones on first- to third-order headwater streams in southern New England, USA. *Forest Ecology and Management*, 258(9): 2117–2126.
<https://doi.org/10.1016/j.foreco.2009.08.007>.
10. Bureau of Meteorology, (2020) *Annual (2019) Climate Summary for Greater Sydney*. Australian Government. Available at <http://www.bom.gov.au/climate/current/annual/nsw/archive/2019.sydney.shtml>.
11. Bureau of Meteorology, (2023a) *Water Data Online – South Creek @ Elizabeth Drive*. Australian Government <http://www.bom.gov.au/waterdata/>.
12. Bureau of Meteorology, (2023b) *Climate statistics for Australian locations – Badgerys Creek AWS*. Australian Government http://www.bom.gov.au/climate/averages/tables/cw_067108.shtml.
13. Caccetta, P.A., Chia, J., Collings, S., Devereux, D., Traylen, A., Wu, X. (2019) Greater Sydney Canopy and Thermal Assessment 2014 and 2016, CSIRO Australia: Creation of UrbanMonitor® landcover and surface baselines.
14. Caissie, D. (2006) The thermal regime of rivers: a review. *Freshwater Biology*, 51(8), 1389–1406. <https://doi.org/10.1111/j.1365-2427.2006.01597.x>.

15. Chang, C.R., Li, M.H. and Chang, S.D. (2007) A preliminary study on the local cool-island intensity of Taipei city parks. *Landscape and Urban Planning*, 80(4): 386– 395. <https://doi.org/10.1016/j.landurbplan.2006.09.005>.
16. Department of Environment and Conservation, (2005) *South Creek demonstration site – Western Sydney riparian corridors Erskin park*. NSW Government Available at <https://www.environment.nsw.gov.au/resources/nature/cumberlandPlainSiteSouthcreek.pdf>.
17. Department of Planning and Environment, (2020) *NSW Landuse 2017 v1.2*. New South Wales Government. Available at <https://datasets.seed.nsw.gov.au/dataset/nsw-landuse-2017-v1p2-f0ed>.
18. Department of Planning and Environment, (2022a) *Controlled activities – Guidelines for riparian corridors on waterfront land*. NSW Government. Available at https://water.dpie.nsw.gov.au/__data/assets/pdf_file/0008/386207/licensing_approvals_controlled_activities_riparian_corridors.pdf.
19. Department of Planning and Environment, (2022b) *Western Sydney Aerotropolis Precinct Plan*. New South Wales Government.
20. Dodman, D.B., Hayward, M., Pelling, V., Castan Broto, W., Chow, E., Chu, R., Dawson, L., Khirfan, T., McPhearson, A., Prakash, Y., Zheng, Ziervogel, G. (2022) Cities, Settlements and Key Infrastructure. Climate Change 2022: Impacts, Adaptation, and Vulnerability. Contribution of Working Group II to the Sixth Assessment Report of the Intergovernmental Panel on Climate Change. *Cambridge University Press*, Cambridge, UK and New York, NY, USA: 907-1040, <https://doi.org/10.1017/9781009325844.008>.
21. Du, H., Song, X., Jiang, H., Kan, Z., Wang, Z. and Cai, Y. (2016) Research on the cooling island effects of water body: A case study of Shanghai, China. *Ecological Indicators*, 67: 31–38. <https://doi.org/10.1016/j.ecolind.2016.02.040>.
22. Dufour, S., Rodríguez-González, P. M., and Laslier, M. (2019) Tracing the scientific trajectory of riparian vegetation studies: Main topics, approaches and needs in a globally changing world. *The Science of the Total Environment*, 653: 1168–1185. <https://doi.org/10.1016/j.scitotenv.2018.10.383>.
23. Dugdale, S. J., Hannah, D. M. and Malcolm, I. A. (2020) An evaluation of different forest cover geospatial data for riparian shading and river temperature modelling. *River Research and Applications*, 36(5): 709–723. <https://doi.org/10.1002/rra.3598>.
24. Elgendawy, a., Davies, P., Chang, H. (2020) Planning for cooler cities: a plan quality evaluation for Urban Heat Island consideration, *Journal of Environmental Policy and Planning*, 22(4): 531-553, <https://doi.org/10.1080/1523908X.2020.1781605>.
25. Eskelson, B. N., Anderson, P. D., Hagar, J. C. and Temesgen, H. (2011) Geostatistical modelling of riparian forest microclimate and its implications for sampling. *Canadian Journal of Forest Research*, 41(5): 974–985. <https://doi.org/10.1139/x11-015>
26. Evans, E. C., McGregor, G. and Petts, G. E. (1998) River energy budgets with special reference to riverbed processes, *Hydrological Processes*, 12: 575–595.
27. Fan, H., Yu, Z., Yang, G., Liu, T. Y., Liu, T. Y. and Hung, C. H., et al. (2019) How to cool hot humid (Asian) cities with urban trees? An optimal landscape size perspective. *Agricultural and Forest Meteorology*, 265: 338–348.
28. Frumkin, H., Bratman, G. N., Breslow, S. J., Cochran, B., Kahn, J., Lawler, J. J., Wood, S. A. (2017) Nature Contact and Human Health: A Research Agenda. *Environmental Health Perspectives*, 125(7): 075001–075001. <https://doi.org/10.1289/EHP1663>.

29. GRASS Development Team, (2015) Geographic Resources Analysis Support System (GRASS GIS) Software, Version 7.1; Open-Source Geospatial Foundation. retrieved from <http://grass.osgeo.org>.
30. Greater Sydney Commission, (2018a) *Western City district plan*. Sydney: GSC
31. Greater Sydney Commission, (2018b) *A metropolis of three cities*. Sydney: GSC.
32. Greenberg, J. A., Hestir, E. L., Riano, D., Scheer, G. J. and Ustin, S. L. (2012) Using LiDAR Data Analysis to Estimate Changes in Insolation Under Large-Scale Riparian Deforestation 1: Using lidar Data Analysis to Estimate Changes in Insolation Under Large-Scale Riparian Deforestation. *Journal of the American Water Resources Association*, 48(5): 939–948. <https://doi.org/10.1111/j.1752-1688.2012.00664.x>.
33. Gunawardena, K. R., Wells, M. J., and Kershaw, T. (2017) Utilising green and bluespace to mitigate urban heat island intensity. *The Science of the Total Environment*, 584-585: 1040–1055. <https://doi.org/10.1016/j.scitotenv.2017.01.158>.
34. Hadi, S. J. and Tombul, M. (2018) Comparison of Spatial Interpolation Methods of Precipitation and Temperature Using Multiple Integration Periods. *Journal of the Indian Society of Remote Sensing*, 46, 1187–1199. <https://doi.org/10.1007/s12524-018-0783-1>
35. Hardin, P. J. and Jensen, R. R. (2007) The effect of urban leaf area on summertime urban surface kinetic temperatures: a Terre Haute case study. *Urban Forestry and Urban Greening*, 6: 63–72.
36. Hofierka, J. and Suri, M. (2002) The solar radiation model for open-source GIS: implementation and applications. Proceedings of the Open-Source GIS-GRASS Users Conference, pp. 1–19
37. Jackson, F. L., Hannah, D. M., Ouellet, V. and Malcolm, I. A. (2021) A deterministic river temperature model to prioritize management of riparian woodlands to reduce summer maximum river temperatures. *Hydrological Processes*, 35(8). <https://doi.org/10.1002/hyp.14314>
38. Jackson, F. L., Hannah, D. M., Ouellet, V. and Malcolm, I. A. (2021) A deterministic river temperature model to prioritize management of riparian woodlands to reduce summer maximum river temperatures. *Hydrological Processes*, 35(8). <https://doi.org/10.1002/hyp.14314>
39. Jaganmohan, M., Knapp, S., Buchmann, C. M. and Schwarz, N. (2016) The Bigger, the Better? The Influence of Urban Green Space Design on Cooling Effects for Residential Areas. *Journal of Environmental Quality*, 45(1): 134–145. <https://doi.org/10.2134/jeq2015.01.0062>.
40. Ji, P., Zhu, C. Y., Wang, H. Y. and Li, S. H. (2013) Effect of Different Width of Urban River on Air Temperature and Relative Humidity of Riverside Greenbelts in Four Seasons. *Chinese Mecial Journal*, 11(2): 240–245.
41. Jiang, Y., Jiang, S. and Shi, T. (2020) Comparative Study on the Cooling Effects of Green Space Patterns in Waterfront Build-Up Blocks: An Experience from Shanghai. *International Journal of Environmental Research and Public Health*, 17(22): 8684–. <https://doi.org/10.3390/ijerph17228684>.
42. Johnson, M. F. and Wilby, R. L. (2015) Seeing the landscape for the trees: Metrics to guide riparian shade management in river catchments. *Water Resources Research*, 51(5): 3754–3769. <https://doi.org/10.1002/2014WR016802>.
43. Justice, C., White, S. M., McCullough, D. A., Graves, D. S. and Blanchard, M. R. (2017) Can stream and riparian restoration offset climate change impacts to salmon populations? *Journal*

- of Environmental Management*, 188(C): 212–227.
<https://doi.org/10.1016/j.jenvman.2016.12.005>.
44. Justice, C., White, S. M., McCullough, D. A., Graves, D. S. and Blanchard, M. R. (2017) Can stream and riparian restoration offset climate change impacts to salmon populations? *Journal of Environmental Management*, 188(C): 212–227.
<https://doi.org/10.1016/j.jenvman.2016.12.005>.
 45. Kim, S. W. and Brown, R. D. (2021) Urban heat island (UHI) intensity and magnitude estimations: A systematic literature review. *The Science of the Total Environment*, 779: 146389–146389. <https://doi.org/10.1016/j.scitotenv.2021.146389>.
 46. Kjellstrom, T., Lemke, B., and Venugopal, V. (2013) Occupational Health and Safety Impacts of Climate Conditions. *Earth Systems and Environmental Sciences*, 1: 145-156.
 47. Kong, F., Yin, H., James, P., Hutyra, L. R. and He, H. S. (2014) Effects of spatial pattern of greenspace on urban cooling in a large metropolitan area of eastern China. *Landscapes and Urban Planning*, 128: 35–47.
 48. Kristensen, P. B., Kristensen, E. A., Riis, T., Alnoee, A. B., Larsen, S. E., Verdonshot, P. F. M. and Baattrup-Pedersen, A. (2015) Riparian forest as a management tool for moderating future thermal conditions of lowland temperate streams. *Inland Waters*, 5(1), 27–38.
<https://doi.org/10.5268/IW-5.1.751>.
 49. Li, G., Jackson, C. R. and Kraseski, K. A. (2012) Modelled riparian stream shading: agreement with field measurements and sensitivity to riparian conditions. *J. Hydrological Processes* 428: 142–151.
 50. Liang, A., Xie, C., and Che, S. (2021) A Study on Microclimate characteristics and energy balance within near-river riparian systems. IOP Conference Series. *Earth and Environmental Science*, 821(1): 12022–. <https://doi.org/10.1088/1755-1315/821/1/012022>.
 51. Loicq, P., Moatar, F., Jullian, Y., Dugdale, S. J. and Hannah, D. M. (2018) Improving representation of riparian vegetation shading in a regional stream temperature model using LiDAR data. *The Science of the Total Environment*, 624: 480–490.
<https://doi.org/10.1016/j.scitotenv.2017.12.129>.
 52. Mathew, A., Khandelwal, S. and Kaul, N. (2017) Investigating spatial and seasonal variations of urban heat island effect over Jaipur city and its relationship with vegetation, urbanization and elevation parameters. *Sustainable Cities and Society* 35: 157–177.
<https://doi.org/10.1016/j.scs.2017.07.013>.
 53. McEvoy, D., Ahmed, I., and Mullett, J. (2012) The impact of the 2009 heat wave on Melbourne’s critical infrastructure. *Local Environment*, 17(8): 783–796.
<https://doi.org/10.1080/13549839.2012.678320>.
 54. McKechnie, A. E., and Wolf, B. O. (2010) Climate change increases the likelihood of catastrophic avian mortality events during extreme heat waves. *Biology Letters* (2005), 6(2), 253–256. <https://doi.org/10.1098/rsbl.2009.0702>.
 55. Mirabi, E., and Davies, P. J. (2022) A systematic review investigating linear infrastructure effects on Urban Heat Island (UHI/ULI) and its interaction with UHI typologies. *Urban Climate*, 45, 101261–. <https://doi.org/10.1016/j.uclim.2022.101261>.
 56. Montazeri, H., Toparlar, Y., Blocken, B., Hensen, J., (2017) Simulating the cooling effects of water spray systems in urban landscapes: a computational fluid dynamics study in Rotterdam, the Netherlands. *Landscapes and Urban Planning*. 159: 85–100.

57. Moore, R., Spittlehouse, D. and Story, A. 2005. Riparian microclimate and stream temperature response to forest harvesting: a review. *Journal of the American Water Resources Association*, 41(4): 813–834. <https://doi.org/10.1111/j.1752-1688.2005.tb04465.x>.
58. Murakawa, S., Sekine, T., Narita, K.-i. and Nishina, D. (1991) Study of the effects of a river on the thermal environment in an urban area. *Energy and Buildings*, 16(3-4): 993-1001.
59. National Research Council. (2002) Riparian Areas: Functions and Strategies for management. Washington, DC: The National Academies Press. <https://doi.org/10.17226/10327>.
60. Office of Environment and Heritage. (2014) Metropolitan Sydney: climate change snapshot. Sydney: NSW Government. Available at: <https://www.climatechange.environment.nsw.gov.au/sites/default/files/2021-06/Metropolitan%20Sydney%20climate%20change%20snapshot.pdf>.
61. Office of Environment and Heritage. (2015) Heatwaves: climate change impact snapshot. Sydney: NSW Government. Available at: <https://www.climatechange.environment.nsw.gov.au/sites/default/files/2021-06/Heatwaves%20Climate%20Change%20Impact%20Snapshot.pdf>.
62. Oke, T.R., (1973) City Size and the Urban Heat Island. *Atmospheric Environment* (1967), 769–779.
63. Oldén, A., Peura, M., Saine, S., Kotiaho, J. S. and Halme, P. (2019) The effect of buffer strip width and selective logging on riparian forest microclimate. *Forest Ecology and Management*, 453: 117623–. <https://doi.org/10.1016/j.foreco.2019.117623>.
64. Olson, D. H., Anderson, P. D., Frissell, C. A., Welsh Jr., H. H. and Bradford, D.F., (2007) Biodiversity management approaches for stream-riparian areas: perspectives for Pacific Northwest headwater forests, microclimates, and amphibians. *Ecological Management*. 246: 81–107.
65. Osmond, P. and Sharifi, E. (2017) *Guide to Urban Cooling Strategies*; Cooperative Research Centres for Low Carbon Living Ltd. Department of Industry, Innovation and Science: Canberra, Australia.
66. Palmer, M. A., Hondula, K. I. and Koch, B. J. (2014) Streams and Rivers: shifting strategies and shifting goals. *The Annual Review of Ecology, Evolution, and Systematics*, 45: 247-249.
67. Park, C. Y., Lee, D. K., Asawa, T., Murakami, A., Kim, H. G., Lee, M. K., and Lee, H. S. (2019). Influence of urban form on the cooling effect of a small urban river. *Landscape and Urban Planning*, 183: 26–35. <https://doi.org/10.1016/j.landurbplan.2018.10.022>.
68. Poole, G. C. and Berman, C. H. (2001) An ecological perspective on in-stream temperature: natural heat dynamics and mechanisms of human-caused thermal degradation. *Environmental Management*. 27 (6): 787-802.
69. Richardson, J. S., Naiman, R. J., Swanson, F. J. and Hibbs, D. E. (2005) Riparian communities associated with Pacific Northwest headwater streams: Assemblages, processes, and uniqueness. *American Water Resource Association*, 41: 935–947.
70. Rocha, A. D., Vulova, S., Meier, F., Förster, M. and Kleinschmit, B. (2022) Mapping evapotranspirative and radiative cooling services in an urban environment. *Sustainable Cities and Society*, 85: 104051–. <https://doi.org/10.1016/j.scs.2022.104051>.
71. Rykken, J. J., Moldenke, A. R. and Olson, D. H., (2007b) Headwater riparian forest-floor communities associated with alternative forest management practices. *Ecological Applications*, 17: 1168–1183.

72. Rykken, J., Chan, S. and Moldenke, A. (2007a) Headwater Riparian Microclimate Patterns under Alternative Forest Management Treatments. *Forest Science*, 53(2): 270–280.
73. Sabo, J. L., Sponseller, R. and Dixon, M., et al., (2005) Riparian zones increase regional species richness by harboring different, not more, species. *Ecology*, 86: 56– 62.
74. Santamouris, M., Haddad, S., Fiorito, F., Osmond, P., Ding, L., Prasad, D. and Wang, R. (2017). Urban Heat Island and Overheating Characteristics in Sydney, Australia. An Analysis of Multiyear Measurements. *Sustainability*, 9(5): 712–. <https://doi.org/10.3390/su9050712>.
75. Sinokrot B. A. and Stefan H. G. (1994) Stream water temperature sensitivity to weather and bed parameters. *ASCE, Journal of Hydraulic Engineering*, 120: 722–736.
76. Smith K. 1972. River water temperatures: an environmental review. *Scottish Geographical Magazine*, 88: 211–220.
77. Solcerova, A., van de Ven, F., Wang, M., Rijdsdijk, M., van de Giesen, N., (2017) Do green roofs cool the air? *Building and Environment*, 111: 249–255.
78. Spatial Services, Department of Customer Service, (2016) NSW Hydrography. *NSW Government*, Available at <https://datasets.seed.nsw.gov.au/dataset/nsw-hydrography>.
79. Sun, Y., Gao, C., Li, J., Li, W. and Ma, R. (2018) Examining urban thermal environment dynamics and relations to biophysical composition and configuration and socio-economic factors: a case study of the Shanghai metropolitan region. *Sustainable Cities and Society*, 40: 284–295. <https://doi.org/10.1016/j.scs.2017.12.004>.
80. Sweeney, B. W., and Newbold, J. D. (2014) Streamside Forest Buffer Width Needed to Protect Stream Water Quality, Habitat, and Organisms: A Literature Review. *Journal of the American Water Resources Association*, 50(3): 560–584. <https://doi.org/10.1111/jawr.12203>.
81. Syafii, N. I., Ichinose, M., Wong N., Kumakura, E., Jusuf, S. K. and Chigusa, K. (2016) Experimental Study on the Influence of Urban Water Body on Thermal Environment at Outdoor Scale Model. *Procedia Engineering*, 169: 191-198.
82. Theeuwes, N. E., Solcerova, A. and Steeneveld, G. J. (2013) Modelling the influence of open water surfaces on the summertime temperature and thermal comfort in the city. *Journal of Geophysical Research: Atmospheres*, 118(16): 8881-8896.
83. Thompson, R. and Parkinson, S. (2011) Assessing the local effects of riparian restoration on urban streams. *New Zealand Journal of Marine and Freshwater Research*, 45(4): 625-636, DOI: 10.1080/00288330.2011.569988.
84. Tsai, C.W., Young, T., Warren, P. H. and Maltby, L. (2017) Riparian thermal conditions across a mixed rural and urban landscape. *Applied Geography (Sevenoaks)*, 87: 106–114. <https://doi.org/10.1016/j.apgeog.2017.07.009>.
85. Voogt, J. A., Oke, T. R. (2003) Thermal remote sensing of urban climates. *Remote Sensing of Environment*, 86: 370–384.
86. Walsh, C. J. (2004) Protection of in-stream biota from urban impacts: minimise catchment imperviousness or improve drainage design? *Marine and Freshwater Research*, 55: 317-326.
87. Walsh, C. J., Roy, A. H., Feminella, J. W., Cottingham, P. D., Groffman, P. M., Morgan II, R. P. (2005) The urban stream syndrome: current knowledge and the search for a cure. *Journal of the North American Benthological Society* 24: 706-723.
88. Wawrzyniak, V., Allemand, P., Bailly, S., Lejot, J. and Piégay, H. (2017) Coupling LiDAR and thermal imagery to model the effects of riparian vegetation shade and groundwater inputs on summer river temperature. *The Science of the Total Environment*, 592:616–626. <https://doi.org/10.1016/j.scitotenv.2017.03.019>.

89. Webb B. W. and Zhang Y. (1999) Water temperatures and heat budgets in Dorset chalk water courses. *Hydrological Processes*, 13: 309–321.
90. Weng, Q., Rajasekar, U., Hu, X., (2011) Modelling urban heat islands and their relationship with impervious surface and vegetation abundance by using ASTER images. *Geoscience and Remote Sensing*, 49, 4080–4089.
91. Williams, S. E., Bolitho, E. E., and Fox, S. (2003) Climate change in Australian tropical rainforests: an impending environmental catastrophe. Proceedings of the Royal Society. *Biological Sciences*, 270(1527): 1887–1892. <https://doi.org/10.1098/rspb.2003.2464>.
92. Yu, Z., Yang, G., Zuo, S., Jørgensen, G., Koga, M., Vejre, H. (2020) Critical review on the cooling effect of urban blue-green space: A threshold-size perspective. *Urban Forestry and Urban Greening*, 49: 126630–. <https://doi.org/10.1016/j.ufug.2020.126630>.